

**Building Bridges between Halide Perovskite Nanocrystals  
and Thin-Film Solar Cells**

Journal:	<i>Sustainable Energy &amp; Fuels</i>
Manuscript ID	SE-PER-07-2018-000315.R1
Article Type:	Perspective
Date Submitted by the Author:	27-Aug-2018
Complete List of Authors:	Yang, Hanjun; Brown University , Chemistry Zhang, Yi; Brown University School of Engineering Hills-Kimball, Katie; Brown University, Chemistry Zhou, Yuanyuan; Brown University, School of Engineering chen, ou; Brown University, Chemistry

Received 00th January 20xx,

Accepted 00th January 20xx

DOI: 10.1039/x0xx00000x

www.rsc.org/

## Building Bridges between Halide Perovskite Nanocrystals and Thin-Film Solar Cells

Hanjun Yang,<sup>#,a</sup> Yi Zhang<sup>#,b</sup>, Katie Hills-Kimball,<sup>a</sup> Yuanyuan Zhou<sup>\*,b</sup> and Ou Chen<sup>\*,a</sup>

The development of halide perovskite (HP) based thin film solar cells has been unprecedentedly in the past few years, and there is significant ongoing effort aiming to make perovskite solar cells (PSCs) more efficient and stable. Parallel to the PSC research, there is growing interest in exploring the synthesis and physicochemical behaviors of HP nanocrystals (NCs). While these HP NCs inherently possess many unique properties that are suitable for the use in PSCs, the reported effort of incorporating the HP NCs into PSCs is still highly limited. As a result, there is a gap between HP NC and PSC research. In this context, we provide here a brief review on the established HP NC synthesis and a discussion on the several recent studies pertaining to the use of HP NCs in PSCs. Based on these, we provide perspectives on promising directions for bridging the gap between the HP NC and PSC research in the future.

### 1. Introduction

Halide perovskites (HPs) have been introduced recently as a new generation of semiconductor materials in the field of optoelectronics. In general, HPs exhibit a three-dimensional (3D) (pseudo-)cubic crystal structure with chemical formula  $ABX_3$ , where A is methylammonium ( $CH_3NH_3^+$  or  $MA^+$ ), formamidinium ( $HC(NH_2)_2^+$  or  $FA^+$ ) or  $Cs^+$ , B is  $Pb^{2+}$ ,  $Sn^{2+}$  or  $Ge^{2+}$ , and X is  $I^-$ ,  $Br^-$  or  $Cl^-$  (Fig. 1).<sup>1–6</sup> The HP family has also been later extended to embrace lower-dimensional (2D, 1D and 0D) perovskites and their variants with accordingly varied chemical formulas ( $A_2BX_4$ ,  $ABX_4$ ,  $A_3B_2X_9$ ,  $A_4BX_6$ , etc.).<sup>7–14</sup> Within 10 years of rapid development, HPs have shown great potential in a wide range of optoelectronic applications such as solar cells, light-emitting devices (LEDs), lasing, photodetectors, and X-ray imaging.<sup>15–24</sup> Most notably, HP-based thin-film solar cells have emerged as revolutionary photovoltaic (PV) technologies that combine the merits of low materials/processing cost and high power conversion efficiency (PCE). Within a very short period of time, the PCE of perovskite solar cells (PSCs) has ramped up to 23.3% since its initial invention by Kojima *et al.* in 2009.<sup>25–27</sup> The swift increase in PCE is not only attributed to the unique

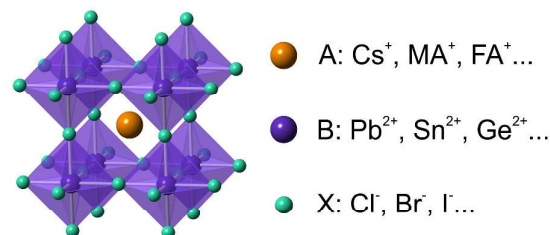


Figure 1. Schematic illustration of crystal structure and typical compositions of halide perovskites.

intrinsic properties of HP materials that include high absorption coefficients,<sup>28</sup> suitable bandgaps,<sup>27,28</sup> long and balanced charge-carrier diffusion-lengths,<sup>31,32</sup> but also due to the unprecedented effort in optimizing HP bulk thin film formation<sup>33–37</sup> and device architectures.<sup>38–40</sup> In parallel with these significant PSC developments, there is rapid growth of interest in exploring the synthesis and properties of HP nanocrystals (NCs). Compared with conventional inorganic semiconductor NCs, HP NCs exhibit many advantageous features, such as high photoluminescence quantum yields (PLQYs),<sup>41,42</sup> narrow emission profiles, facile bandgap tunability,<sup>43,44</sup> as well as extreme ease in both their direct synthesis and post-synthetic treatments.<sup>45–47</sup> While these HP NCs have been widely studied for display and light-emitting applications,<sup>48–51</sup> there is much less effort being devoted to applying HP NCs in PSCs. In fact, merits of HP NCs including superior particle dispersity in non-polar solvents,<sup>52</sup> ultralow defect density,<sup>53,54</sup> and uniformities in crystal size and

<sup>a</sup> Department of Chemistry, Brown University, Providence, RI 02912, USA. Email: ouchen@brown.edu

<sup>b</sup> School of Engineering, Brown University, Providence, RI 02912, USA. Email: yuanyuan\_zhou@brown.edu

<sup>#</sup> These authors contributed equally to this work.

<sup>†</sup> Electronic Supplementary Information (ESI) available: [details of any supplementary information available should be included here]. See DOI: 10.1039/x0xx00000x

morphology,<sup>55,56</sup> render them inherently suitable for the integration in PSCs.<sup>57,58</sup> However, to date, these merits have not been sufficiently explored for PV applications. In this context, the current gap between HP NC and PSC research needs to be filled.

In this article, a brief review of direct synthetic routes and post-synthetic tuning strategies for HP NCs that can enable composition/structure controls is first presented. Then, recent studies on applying HP NCs to PSC device modification and fabrication are summarized. Finally, we provide our perspectives on the future research directions that may further bridge the gap between HP NC synthesis and post-treatment and their PSC applications. The objective of this perspective article is not only to highlight many promising possibilities that HP NCs are capable to offer for making efficient, stable and versatile PSCs, but also stimulate interdisciplinary researchers to further explore this young but fascinating research area.

## 2. Synthesis and Properties of HP NCs

### Synthesis of HP NCs

High-quality semiconductor NCs (also known as quantum dots, QDs) are the building blocks and vital basis in not only fundamental research, but also a spectrum of technological applications.<sup>59–64</sup> The first demonstration of a solution synthesis of HP NCs was reported in 2014 by Schmidt *et al.*, where they synthesized methylammonium lead bromide (MAPbBr<sub>3</sub>) hybrid organic-inorganic HP NCs using a non-templating antisolvent precipitation method.<sup>65</sup> Soon afterwards, this synthetic method was optimized by Zhang *et al.* who pioneered using a miscible solvent/antisolvent combination (*e.g.*, dimethylformamide (DMF) and toluene) for making high-quality MA-based hybrid HP NCs with much improved optical properties.<sup>66</sup> This so-called ligand-assisted reprecipitation (LARP) synthetic method relies on a dramatic change in solvent polarity by adding a miscible antisolvent to initiate rapid HP nucleation in solution (Fig 2a,b). The subsequent NC growth and ripening processes can be controlled by long-chain organic ligands added to the reaction solution. Applying this LARP method, a wide range of high-quality HP NCs can be synthesized.<sup>67–69</sup> Arguably, the most beneficial aspect of the LARP synthesis is the use of ambient reaction conditions (*i.e.*, room temperature, commercially available chemicals), which enables the use of low-boiling-point solvents and chemicals, thus offering the promise of large-scale industrial-level production.<sup>70</sup> In addition, the general ease of dissolving non-lead metal precursors (*e.g.*, bismuth halide, silver nitrate) in coordinating solvents makes the LARP procedure attractive for synthesizing Pb-free HP NCs.<sup>71,72</sup> Although the LARP method tends to result in small NCs with an average diameter < 5 nm, larger NCs can be achieved through changing the reaction temperature and solvents.<sup>41,73</sup> However, the low solubility of common inorganic 'A' cation precursors (*e.g.*, Cs salts) in organic solvents (*e.g.*, DMF, dimethyl sulfoxide (DMSO)) limits the generalization of

the LARP procedure for fabrication of all-inorganic Cs-based HP NCs.

The hot-injection method, which is a state-of-the-art strategy for conventional NC synthesis, has been quickly adapted for the synthesis of all-inorganic HP NCs. The first example was reported by Protesescu *et al.* using 1-octadecene (ODE) as a solvent, PbBr<sub>2</sub> and Cs-oleate as precursors, and oleic acid and oleylamine as capping ligands.<sup>74</sup> Uniform CsPbX<sub>3</sub> nanocubes with a tunable edge lengths from 3.8 to 11.8 nm were synthesized using the hot-injection technique at temperatures ranging from 140 to 200 °C (Fig. 2c-e). Mixed halide NCs with precise halide ratios can be easily synthesized using a mixture of PbX<sub>2</sub> precursors. While the general format of synthesis remains nearly unchanged, recent improvements have been made to ensure better NC monodispersity using active precursors and optimized reaction conditions.<sup>55,75,76</sup> Low-dimensional HP NCs are defined as HP NCs with the same crystal structure, but containing at least one dimension that is small in size. The hot-injection method is particularly suitable for the synthesis of low-dimensional HP NCs, such as nanowires and nanoplatelets (Fig. 3a, b).<sup>77–81</sup> These low-dimensional NCs are typically sensitive to polar solvents, which makes the use of the LARP synthesis very challenging. Monodispersed thickness control of nanoplatelets and nanowires are readily achieved by controlling the nucleation and growth kinetics by manipulating ligands, temperature, and precursor ratio.<sup>82</sup> The uniformity of as-synthesized NCs can be illustrated by their tendency to form ordered superlattices (Fig. 3c, d).<sup>83–85</sup> Beyond inorganic HP NCs, the hot-injection technique can be adopted for the synthesis of hybrid organic-

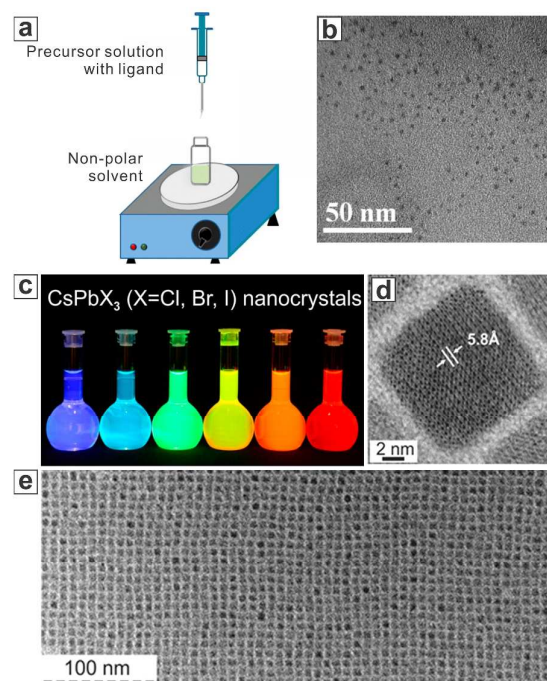


**Figure 2.** (a) Schematic image for the procedure of ligand-assisted reprecipitation (LARP). (b) Transmission electron microscopy (TEM) images for MAPbBr<sub>3</sub> NCs synthesized by LARP. (c) Optical images of CsPbX<sub>3</sub> nanocubes synthesized by the hot injection method under UV light. (d,e) TEM images of CsPbX<sub>3</sub> nanocubes. (a,b) are reproduced from ref. 66 with permission of American Chemistry Society. (c-e) are reproduced from ref. 74 with permission of American Chemistry Society

inorganic HPs NCs, such as  $\text{FAPbX}_3$ .<sup>56,86</sup> The low boiling point of certain organic precursors however, limits the use of hot-injection for some hybrid HP NCs syntheses (e.g.,  $\text{MAPbX}_3$ ). Another drawback of the hot-injection technique is the use of high-boiling-point solvents with long organic hydrocarbon chains, such as ODE. These high-boiling-point solvents, together with organic ligands, may affect the uniformity and conductivity of the resultant HP NC thin film, thus limiting the final device performance. In this context, multiple rounds of purifications are required to remove these insulating components. This is challenging for HP NCs because of their instability upon interaction with polar solvents that are commonly used in purification procedures. The study of optimized purification procedure without causing aggregation or phase transition is crucial for the incorporation of HP NCs in optoelectronic devices.

Alternative synthetic routes offer supplementary improvements in certain aspects as compared with the aforementioned two methods. For example, a solvothermal method initiates the reaction at a mild temperature and a high pressure. The controlled nucleation and growth results in novel particle morphologies, including nanorods or nanosheets.<sup>87,88</sup> Top-down techniques, such as mechanochemical exfoliation methods, generally reduce the use of hazardous reagents or high-boiling-point species, rendering them as greener substitutes for large-scale productions.<sup>89–92</sup>

#### Phase stability

HPs materials are notorious for having a variety of polymorphs. The cubic phases, which are only stable at elevated temperatures, have the highest absorption efficiency and optimal optical properties. Other phases with lower symmetries are more stable at room temperature, at the stake of larger bandgaps and undesired optoelectronic properties.<sup>93,94</sup> Therefore, special synthetic techniques and post-synthetic treatments are often needed to obtain and preserve the cubic phase at room temperature. As we have discussed in the previous section, HP NCs in cubic phase can be readily synthesized due to the rapid kinetic during injection as well as the surface effects. However, being meta-stable at room temperature, cubic HPs tend to transform into the phases with lower symmetries in ambient conditions, especially for I-containing perovskites. The transformation can be enhanced by light, oxygen, moisture and polar organic solvents.<sup>95,96</sup>

While encapsulating the HP NCs with polymer, silica or glass can significantly stabilize the cubic phase, the resultant decrease in conductivity renders NCs produced in this manner unfit for photovoltaic application.<sup>97–99</sup> Alternatively, stabilizing a desirable phase via compositional optimization has been heavily investigated. The relative abundance of halide anions is especially important for the stability of HP NCs.<sup>100,101</sup> The stabilizing effect was attribute to the surface abundance of lead-halide layer, which isolate the perovskite 'core' from the environment. By alloying HP NCs with ions of varying sizes, it is possible to adjust the Goldschmidt tolerance factor of

perovskite<sup>102</sup> and therefore achieve higher stability for the cubic phase. For example, in I-based HPs, Cs is too small to support cubic phases while FA is too large. Protesescu *et al.* synthesized Cs-FA mixed HP NCs via a hot-injection method with both high phase stability and high PL QY even after 6-month storage in ambient condition.<sup>86</sup> However, their mixing range was limited to the Cs-rich end, which resulted in an unfavourable bandgap. In addition to the tolerance factor adjustment, mixing ions offers a higher entropy for the cubic phase and therefore an increased phase stability.<sup>103</sup>

#### Bandgap tunability

Bandgap is the determining parameter for semiconductor materials. Semiconductors with different bandgaps can have different functions in PSCs (absorbers, interface modifiers, etc.). The wide bandgap tunability that HP NCs offer is of vital importance for their flexible functions in PSCs.

The density of states DFT calculations have shown that the valance band (VB) of HP materials mainly comprises of halide p orbitals, while the conduction band (CB) is dominated by 'B' cation frontier s and p orbitals.<sup>104</sup> As a result, the bandgaps of HP materials are significantly influenced by B cations and halide anions. HP NCs with emission covering the full visible range of 400-730 nm can be achieved by only altering their halide composition ( $\text{Cl} \rightarrow \text{Br} \rightarrow \text{I}$ ) (Fig. 4a).<sup>66</sup> Specifically, as predicted by the Shockley-Queisser limit,<sup>105</sup> the relatively lower bandgaps of I-based HPs make them more ideal absorbers for PSCs than Cl- and Br-based analogues. The full spectrum coverage, ease of exchange, and ability of forming uniform halide alloys make halide composition control the most facile strategy to reach a certain targeted bandgap. Alternatively, adjusting the 'B' cation (e.g., replacing Pb) in HP NCs offers another effective way to alter the electronic

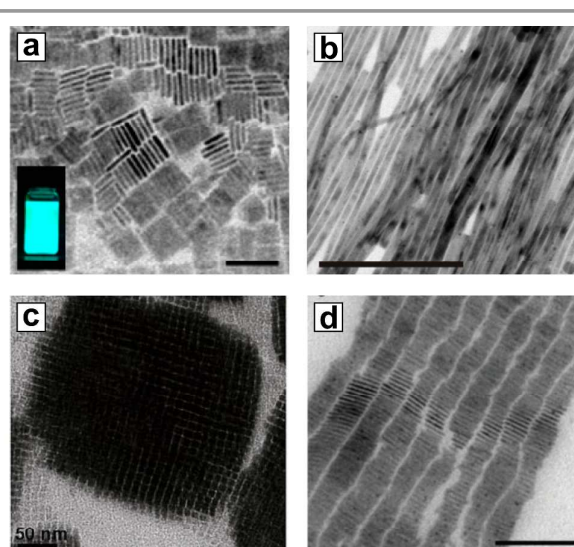
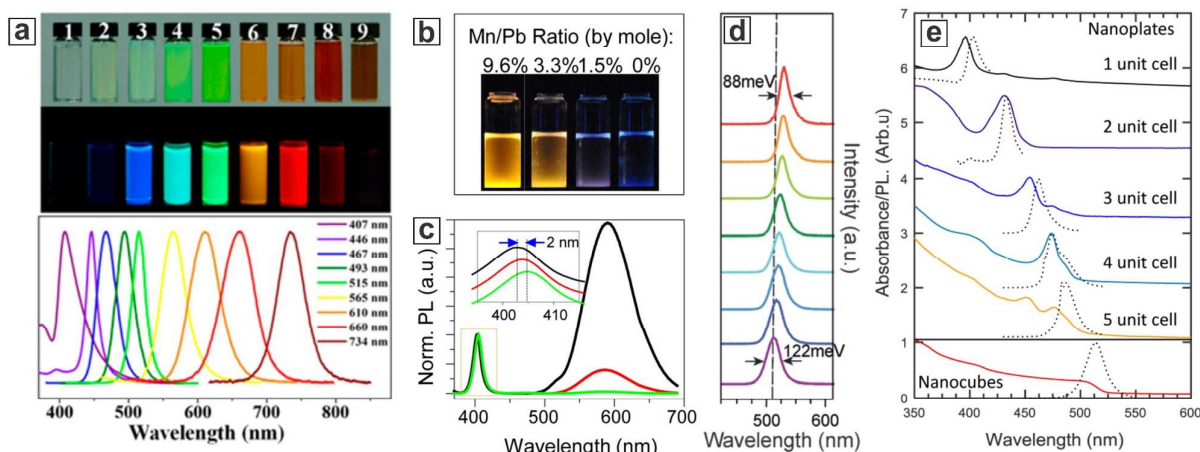


Figure 3. (a,b) TEM images of  $\text{CsPbBr}_3$  nanoplatelets and nanowires. Scale bar = 50 nm and 200 nm, respectively (c,d) TEM images showing self-assembled superstructures for  $\text{CsPbX}_3$  nanocubes and nanoplatelets. Scale bar = 50 nm and 100 nm, respectively. (a) is reproduced from ref. 77 with permission of American Chemistry Society. (b) is reproduced from ref. 79 with permission of American Chemistry Society. (c) is reproduced from ref. 83 with permission of Swiss Chemical Society. (d) is reproduced from ref. 80 with permission of Wiley-VCH.



**Figure 4.** (a) Optical images and PL spectra of MAPbX<sub>3</sub> nanoparticles with different halide composition varying from MAPbCl<sub>3</sub> (left) to MAPbBr<sub>3</sub> (middle) to MAPbI<sub>3</sub> (right). (b,c) Optical images and PL spectra for Mn-doped CsPbCl<sub>3</sub> nanocubes with different doping concentrations. (d) PL spectra of MAPbBr<sub>3</sub> (bottom) to FAPbBr<sub>3</sub> (top) nanocubes during a cation exchange process. (e) Absorption (solid line) and PL spectra (dashed line) for CsPbBr<sub>3</sub> nanoplatelets of atomic thickness precision and nanocubes. (a) is reproduced from ref. 66 with permission of American Chemistry Society. (b,c) are reproduced from ref. 113 with permission of American Chemistry Society. (d) is reproduced from ref. 111 with permission of Royal Society of Chemistry. (e) is reproduced from ref. 77 with permission of American Chemistry Society.

properties, especially within the goal of further narrowing the material bandgap to achieve a better match with the solar spectrum. In this regard, Sn(II) and Ge(II) are the two potential Pb replacements that can reduce the conduction band minimum (CBM) and thus reduce band gaps.<sup>106,107</sup> However, the syntheses of Sn- and Ge-based HP NCs are still challenging due to cation instability caused by further oxidation of Sn(II) to Sn(IV), or Ge(II) to Ge(IV).<sup>108–110</sup> This oxidation problem hinders the related material development. At last, although not direct, the 'A' cation may also affect the bandgap tunability largely by adjusting the lattice parameter, in turn altering the orbital overlap in the VB and CB (Fig 4.d).<sup>111</sup> When all other components are fixed, the bandgaps of bulk HPs show a decreasing trend when the 'A' cation radii increases from Cs (e.g., 1.73 eV for CsPbI<sub>3</sub>) to MA (e.g., 1.57 eV for MAPbI<sub>3</sub>), to FA (e.g., 1.48 eV for FAPbI<sub>3</sub>).<sup>112</sup>

One additional unique advantage of nanoscale HPs for bandgap fine tuning is afforded through the quantum confinement effect. When the size of NCs is scaled down below the material's Bohr radius, the energy levels near the band edge become discrete, resulting in the emergence of multiple absorption features with blue-shifted profiles. Examples of this quantum confinement effect can be found for all types of HP NCs. In particular, I-containing HP NCs show the most dramatic influence due to the large Bohr radii as compared with their Cl and Br counterparts (e.g., 2.5 nm for CsPbCl<sub>3</sub>, 3.5 nm for CsPbBr<sub>3</sub>, 6 nm for CsPbI<sub>3</sub>).<sup>74</sup> As the edge length of CsPbI<sub>3</sub> nanocubes dropped from 12.5 nm to 3.4 nm, the NC PL peak exhibited a large range blue-shift from 670 nm to 585 nm.<sup>57</sup> The quantum confinement effect is especially more profound in low-dimensional HP NCs because they have at least one dimension significantly smaller than the Bohr radii, such as in ultra-thin nanowires and nanoplatelets. As the smallest dimension of these materials approaches a few

atomic layers, adding or subtracting single monolayers results in a drastic change in the photophysical properties.<sup>68,79</sup> For example, Bekenstein *et al.* found that when the thickness of CsPbBr<sub>3</sub> nanoplatelets was changed from one to five monolayers (while maintaining the lateral size) the PL peak could be adjusted from 400 nm to 480 nm (Fig. 4.e).<sup>77</sup> This size/shape induced quantum confinement effect of HP NCs offers a composition-independent approach toward tuning bandgap structure, providing benefits for PSC designs. This includes the possibility of their use in graded bandgap PSCs and in perovskite-perovskite tandem solar cells which cannot be easily accessed through a compositional control due to possible inter-layer ion exchange processes.

#### Doping in HP NCs

The range of metal cations that can form HPs is limited by their valency and ionic sizes. However, it is possible to introduce small amounts of heteroatoms into the HP lattice (also known as doping). The most striking feature of doping is the introduction of extrinsic optoelectronic properties.<sup>106</sup> For example, Mn-doped CsPbCl<sub>3</sub> NCs exhibiting a strong emission centred at around 600 nm were successfully synthesized without significantly altering the crystal structure or the morphology of host NCs (Fig 4b, c).<sup>113–117</sup> In addition to Mn, rare earth ion dopants such as Yb, Eu, Dy and Ce exhibit bright emission with high QYs in CsPbCl<sub>3</sub> HP NCs.<sup>118–120</sup> The large Stokes shifts of dopant emission are beneficial for down-shifting high energy photons (e.g., ultraviolet light) and for reducing the photon reabsorption. Additionally, doping is able to alter bandgaps. For example, by doping Sn, Cd, Zn and Bi cations can cause an increased bandgap in CsPbBr<sub>3</sub> NCs and change the PL dynamics.<sup>46,121</sup> Mn-doped CsPbCl<sub>3</sub> has shown enhanced PL stability compared with their undoped counterparts.<sup>122</sup> While the detailed mechanisms are still under

investigation, doping in HP NCs has shown potentials in solar energy and display related applications.<sup>123,124</sup>

### 3. Post-Synthetic Treatments of HP NCs

The 'soft' nature (*i.e.*, prone to change under external stimulus) of HP NCs enable a number of post-synthetic routes to modify their compositions, crystal structures, surface passivation and electronic properties much beyond what the direct synthetic methods can offer. The development of such modification reactions or techniques has been an active research topic fuelled by exciting discoveries. It allows for optimization of the HP NC-based materials in composition and structure for the sequential use in PSCs. In this section, we discuss three major post-synthetic treatments for HP NCs, which are directly related to the PSC applications. Other post-synthetic treatments such as encapsulation of HP NCs in polymer or silica matrices, and ligand or ion induced crystal phase transformations will not be discussed here. We refer readers to other excellent literature for these related topics.<sup>47,125–131</sup>

#### Ion exchange reaction

The post-synthetic ion exchange method is a powerful tool commonly utilized in nanoscale research to form meta-stable phases and/or heterostructures. As discussed in the previous section, changing the halide anion can dramatically tune the bandgap of HP NCs. Unlike traditional cadmium-chalcogenide-based QDs (*e.g.*, CdSe and CdS QDs), in which anion exchange reactions are limited by their large ionic radii and strong bonding, halide ions in HP NCs can be rapidly exchanged in either colloidal or solid phases even at room temperature.<sup>132,133</sup> Various halide precursors have shown high reactivities during the exchange reactions, including inorganic halide salts, alkyl ammonium halides, and even HP NCs with different halide anions.<sup>43,44,134</sup> This exchange can be achieved by simply mixing the halide precursors with NCs dispersed in their colloid dispersion. HP NCs containing varying halide compositions (except the  $\text{CsPbCl}_{x-1}\text{I}_x$ , which is restricted by large ionic radii difference<sup>43</sup>) can be achieved (Fig 5a).<sup>43,44,135</sup> The final particle stoichiometry is solely determined by the precursor ratio introduced into the reaction because no thermodynamic preference for halide anions has been shown.<sup>136</sup> The high anion compatibility prevented any loss in shape or size during the process of exchange.<sup>137</sup> Although convenient, the fast kinetics of the halide exchange reaction can also be a challenge for NC processing. For example, the uncontrollable halide exchange process hinders the formation of more complex nanostructures, or the coexistence of HP NCs of different halide compositions in colloidal solution.<sup>43</sup> Novel methods have been developed to achieve a controllable exchange process, including photoexcited anion exchange,<sup>138</sup> solid state exchange,<sup>139</sup> or surface-controlled exchange.<sup>140,141</sup>

While the halide exchange is the most common and facile ion exchange reaction, cation exchange is also achievable and important in tuning the HP NC properties.<sup>46,142</sup> Recently, Hills-Kimball *et al.* showed that  $\text{FAPbX}_3$  NCs, which had been

difficult to obtain via direct synthesis routes, can be obtained by cation exchange from  $\text{MAPbX}_3$  HP NCs through a novel 'solid-liquid-solid' exchange process.<sup>111</sup> While the reaction speed is much slower than the halide exchange reactions, complete transformation can be still reached. One advantage of this new 'solid-liquid-solid' reaction setup with slow kinetics is the possibility of intermediate reaction termination at designed mixtures of 'A' cation compositions for desired optical properties.<sup>111</sup> For the 'B' cations, the exchange from Pb to Sn, Cd, Zn has been demonstrated to produce  $\text{CsPb}_{1-x}\text{M}_x\text{Br}_3$ .<sup>46,117,143</sup> As is discussed above, the 'B' cation exchange has a profound influence on the optical properties. In the above system, as large as a 60 nm blueshift in both absorption and PL profiles was observed. This large shift was explained by a lattice contraction effect, which is evidenced by no significant alternations in particle size or shape.

#### Surface ligand engineering

Organic capping ligands play a crucial role in stabilizing NCs in solution. Such ligands are highly dynamic and can be easily lost during the purification process. This loss of ligands can lead to a destabilization of the NCs, thus initiating an undesired Ostwald ripening process.<sup>144</sup> The same ligand loss may also diminish the optical properties of the HP NCs. Therefore, optimized ligand binding and enhanced surface coverage can improve not only the colloidal stability, but also the optical properties of HP NCs. Alkyl amines and alkyl acids are the most common ligands for HP NCs. They can efficiently passivate the NCs, especially when both types of ligands are present.<sup>145,146</sup> In addition, co-passivating the NC surface with short inorganic ligands, *e.g.*, thiocyanate, can further promote the PL QY of HP

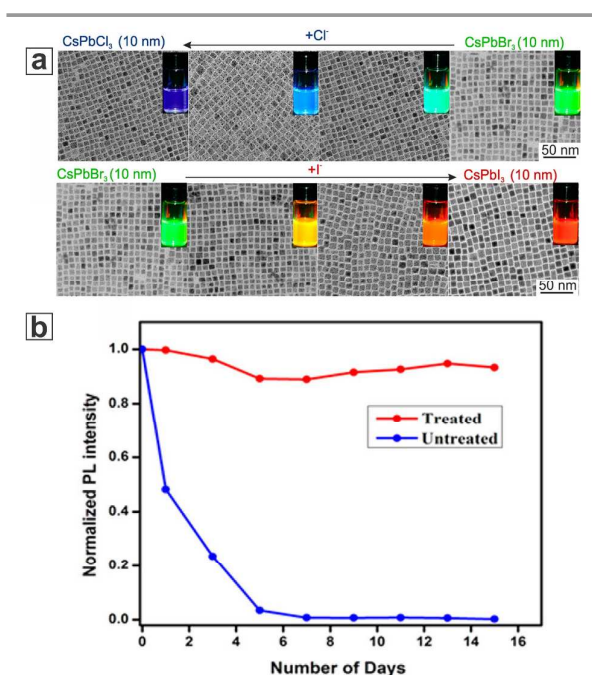


**Figure 5.** (a) TEM and optical images under UV light during a halide exchange reaction of  $\text{CsPbX}_3$  nanocubes. (b) Stability of  $\text{CsPbI}_3$  nanocubes with or without bidentate ligand treatment. (a) is reproduced from ref. 43 with permission of American Chemistry society. (b) is reproduced from ref. 150 with permission of American Chemistry society.

NCs (CsPbI<sub>3</sub> NCs) to approach unity while maintaining a high particle colloidal stability.<sup>147</sup> It was proposed that thiocyanate can penetrate through the bulky organic ligand layer and attach to unsaturated sites on the NC surface, thus offering a high surface passivation efficiency. Moreover, the use of bulky branched ligands or peptides showed a better NC compatibility with protic solvents.<sup>148,149</sup>

Another strategy to stabilize HP NCs involves adjusting the binding form between NCs and ligands. Zwitterionic ligands such as amino acids or amino-sulfonate are able to bind tightly to both cations and anions on the surface of NCs. When capped with zwitterionic ligands, superior properties of HP NCs including a high colloidal solubility (50-100 mg/mL), close-to-unity PL QY, and a high colloidal stability were exhibited.<sup>52</sup> In another example, a bidentate ligand with short carbon chain, 2,2'-iminodibenzoic acid, was installed on the surface of CsPbI<sub>3</sub> NCs. NCs coated with this ligand were not only stable and highly luminescent, but also showed an enhanced conductivity and electroluminescence performance when used in LED (Fig. 5b).<sup>150</sup> The ionic nature and rich crystal phases of the HP NCs result in the capping ligands playing additional roles as opposed to solely serving as a protective layer. For example, excess organo-amine ligands in NC solution can extract Pb cations from HP NCs, resulting in a Pb-deficient trigonal Cs<sub>4</sub>PbX<sub>6</sub> crystal phase with a much wider bandgap and complicated photophysical properties.<sup>47,151</sup> Further increasing the amount of amine ligands may result in a total dissolution of the HP NCs to their ionic forms.

Although HP NCs are initially part of a colloidal solution, they need to be extracted out of solution for PSC device fabrication. While long organic ligands are crucially important in the synthesis and stabilization of HP NCs in solution, these insulating organic molecules are undesirable in optoelectronic devices.<sup>152,153</sup> Hence, these long organic ligands need to be replaced or removed for device fabrication. The replacement of long organic ligands can happen either during the formation of NCs or via a post-synthesis ligand exchange process. For example, short 1-butylamine can serve as the ligand to produce colloidal CsPbBr<sub>3</sub> NCs used for high-voltage solar cells.<sup>70</sup> The produced particles can be directly used to fabricate NC-based conducting films without a lengthy post-synthetic ligand treatment. In another example, a relatively short ligand of didodecylmethylammonium bromide was used to replace oleic acid and oleylamine on CsPbBr<sub>3</sub> NCs after synthesis. LED devices made using these treated NCs exhibited an order of magnitude higher external quantum efficiency (EQE) than that of untreated NCs (3% vs 0.1%).<sup>154</sup> For PSC device fabrication, a total removal of organic ligands by antisolvent washing or salt-induced coarsening is commonly applied to improve film conductivity, which will be further discussed in later sections.<sup>57,155</sup> Studies on ligand effects in NC thin film formation and associated device performances are still limited, leaving room for future research toward the development of a wide range of ligand selection for HP NC-based PSC applications.

### Pressure-treatment of HP NCs

Being an important thermodynamic variable, pressure casts a significant influence on the crystal structures of various materials.<sup>156–162</sup> The dynamic structures of the HP materials promise a structure-property tunability at elevated pressure. Compared with bulk counterparts, the pressure effect on HP NCs has been much less studied. The Chen group reported the first detailed study of pressure processing on self-assembled CsPbBr<sub>3</sub> NC superlattices.<sup>163</sup> Through synchrotron-based *in situ* small/wide angle X-ray scattering (SAXS/WAXS) and optical spectroscopy measurements, the crystal phase transition, superlattice transformation and the optical property evolution were simultaneously monitored. A concurrent crystal phase purification and PL enhancement were reported. *Ex situ* electron microscopy characterizations showed an interesting 2D nanoplatelet formation through a pressure-induced orientated attachment process (Fig. 6a,b). Similar changes in both particle morphology and optical property for MAPbBr<sub>3</sub> NCs under pressure were also demonstrated.<sup>164</sup> Later, a study on the same CsPbBr<sub>3</sub> system was reported from G. Xiao *et al.*, in which a more detailed investigation of the bandgap evolution as a function of pressure was conducted.<sup>165</sup> This pressure processing technique has further been expanded to I-based HP NCs, such as CsPbI<sub>3</sub> and FAPbI<sub>3</sub>, with a bandgap energy range more relevant for PSC applications (Fig 6c).<sup>166–168</sup> Combining with high-pressure studies on perovskite bulk materials,<sup>169–178</sup> it can be concluded that external high-pressure-processing is capable of serving as an efficient and chemically-orthogonal mean to fine tune the crystal structure,

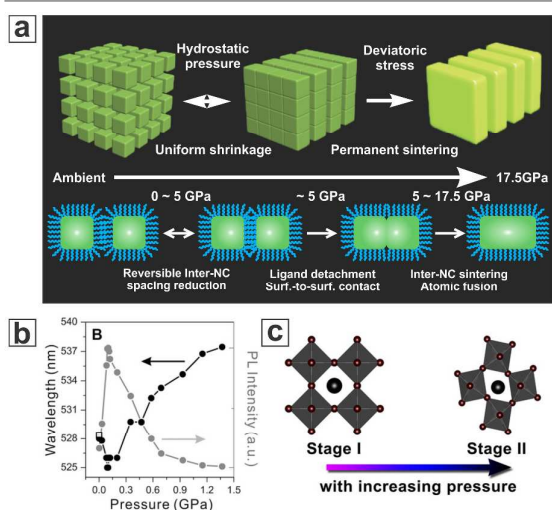


**Figure 6.** (a) Schematic drawing showing the pressure-sintering mechanism for CsPbBr<sub>3</sub> nanocubes into nanoplatelets. (b). PL peak wavelength and intensity for CsPbBr<sub>3</sub> nanocubes with increasing high pressure. (c) Diagram showing the crystal structure transformation of CsPbI<sub>3</sub> from cubic phase to orthorhombic phase with increasing pressure. (a,b) are reproduced from ref. 163 with permission of Wiley VCH. (c) is reproduced from ref. 167 with permission of American Chemistry society.

controllably engineer the bandgap and even generate new perovskite materials overcoming conventional synthetic limitations. Regardless of the promise, how to imitate the required high-pressure environment inside PSC devices remain challenging.

#### 4. HP NCs-Modified Thin-Film PSCs

Great progress in the synthesis and post-synthetic improvement of HP NCs aimed to make them ready for the further incorporation in PSC devices to either modify the HP bulk thin film or to replace it completely. In this section, we will focus our discussion on how the HP NCs improve bulk thin film-based PSC performances through one of the following two ways: (1) smoothing the PV device interfacial band alignment; (2) managing photon propagation using the excitonic properties of HP NCs.

##### Interfacial band alignment modification

The first major utilization of HP NCs for PSCs was to serve as an interface modifier for the HP bulk thin films in order to enhance band energy alignment and device integration. Compared with other modifiers such as polymers,<sup>179</sup> and molecular species,<sup>180–183</sup> HP NCs are unique due to their congeneric nature to the HP bulk thin film absorbers in both the chemical composition and crystal structure. One of the earliest studies regarding the integration of HP NCs as modifiers in PSCs was reported by Cha *et al.*, where an interfacial layer of  $\text{MAPbBr}_{3-x}\text{I}_x$  HP NCs was introduced between the  $\text{MAPbI}_3$  HP bulk thin film and the hole-transporting material (HTM).<sup>184</sup> Here, the  $\text{MAPbBr}_{3-x}\text{I}_x$  HP NCs were dispersed in chlorobenzene and then spin-coated on the as-crystallized  $\text{MAPbI}_3$  HP bulk thin film. It was found that by adjusting the halide ratio in  $\text{MAPbBr}_{3-x}\text{I}_x$  NCs, their VB maximum (VBM) could be tuned to be located between the VBM of  $\text{MAPbI}_3$  bulk thin film absorber and the highest occupied molecular orbital (HOMO) of the HTM. In this context, the hole injection efficiency at the HP/HTM interface was greatly facilitated, resulting in significant improvements in all PV parameters including short-circuit photocurrent ( $J_{SC}$ ), open-circuit voltage ( $V_{OC}$ ) and fill factor (FF). The PSCs made using the HP bulk thin films modified with  $\text{MAPbBr}_{0.9}\text{I}_{2.1}$  HP NCs showed 23% increase in the overall PCE compared with the HP-NC-free case. A following work in a similar topic was later conducted by Zai *et al.*, where  $\text{CsPbBr}_3$  NCs were selected as a model material to be incorporated into the  $\text{FA}_{0.85}\text{MA}_{0.15}\text{Pb}(\text{I}_{0.85}\text{Br}_{0.15})_3$  HP bulk thin film during the antisolvent-dripping process (Fig 7a).<sup>185</sup> In this work, the  $\text{CsPbBr}_3$  NCs induced surface modification occurred along with the formation of the  $\text{FA}_{0.85}\text{MA}_{0.15}\text{Pb}(\text{I}_{0.85}\text{Br}_{0.15})_3$  HP bulk thin film, which was different from the study by Cha *et al.* Without a significant influence on the microstructures of the final  $\text{FA}_{0.85}\text{MA}_{0.15}\text{Pb}(\text{I}_{0.85}\text{Br}_{0.15})_3$  bulk thin film, the incorporation of NCs boosted the PSC performance to an impressive PCE of 19.45%.<sup>185</sup> They attributed the PCE increase to the enhanced charge collection at the NC-modified absorber/HTM interface owing to the formation of a more favourable energy alignment

(Fig 7b, c), which was in line with the conclusion drawn by Cha *et al.*<sup>58</sup>

In a recent study, Zhang *et al.* demonstrated a more complicated NC interfacial modification strategy through incorporation of a HP nanosheet/nanocube bilayer on top of a HP bulk thin film absorber.<sup>186</sup> This proof-of-concept demonstration is solely based on  $\text{CsPbBr}_2$  composition but with different morphologies (*i.e.*, thin film, nanosheet, and nanocube). Their bandgap differences resulting from tuned quantum confinement effect offered a preferred energy alignment in the HP bulk thin film/HTM interface. A high  $V_{OC}$  of 1.19 V was reached in the PSCs using this complex structure. Additionally, a record PCE of 12.39% was reported for the  $\text{CsPbBr}_2$  composition which has a relatively large bandgap of 1.9 eV. This study clearly demonstrated the merits of using HP NCs as modifiers for the PSCs.

##### Photon management

In addition to the interfacial modification using HP NCs on bulk thin films, superior optical properties, especially the PL of HP NCs can also be utilized for improving the PSCs. For example, Wang *et al.* introduced Mn-doped  $\text{CsPbCl}_3$  NCs, which served as a light down conversion layer, onto the illuminated side of  $\text{MAPbI}_3$  bulk thin film PSCs (Fig. 7d).<sup>187</sup> The Mn-doped  $\text{CsPbCl}_3$

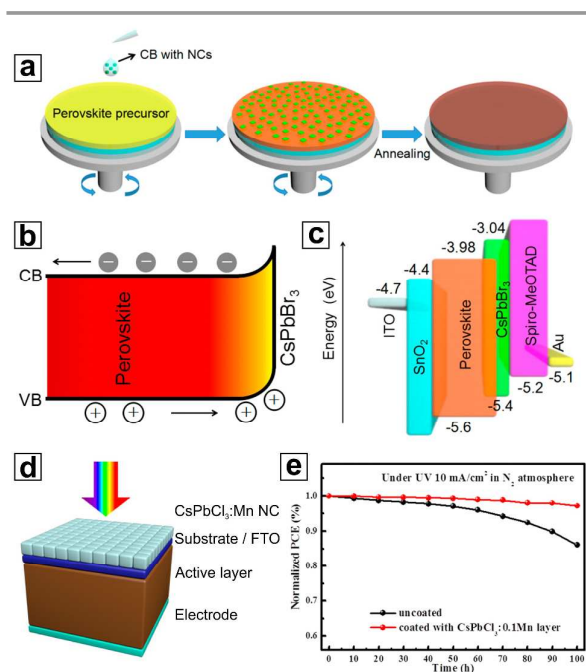


**Figure 7.** (a) Schematic representation of the incorporation of  $\text{CsPbBr}_3$  HP NCs into the  $\text{FA}_{0.85}\text{MA}_{0.15}\text{Pb}(\text{I}_{0.85}\text{Br}_{0.15})_3$  HP thin film during the antisolvent-dripping step of the HP bulk thin film synthesis. (b) Energy-level diagram of the  $\text{FA}_{0.85}\text{MA}_{0.15}\text{Pb}(\text{I}_{0.85}\text{Br}_{0.15})_3$  HP bulk thin film after  $\text{CsPbBr}_3$  NC modification. (c) Schematic diagram of energy levels in the PSCs made using  $\text{FA}_{0.85}\text{MA}_{0.15}\text{Pb}(\text{I}_{0.85}\text{Br}_{0.15})_3$  HP bulk thin films with the  $\text{CsPbBr}_3$  NCs modification, showing a graded heterojunction structure. (d) Schematic structure of solar cells coated with a thin layer of Mn-doped  $\text{CsPbCl}_3$  NCs. (e) Stability comparison of the PSCs with and without a Mn-doped  $\text{CsPbCl}_3$  NC layer under continuous UV irradiation in a  $\text{N}_2$  atmosphere. (a-c) are reproduced from ref. 185 with permission of American Chemistry society. (d,e) are reproduced from ref. 187 with permission of American Chemistry society.

NCs were able to enhance absorption in the UV range of sunlight while remaining transparent in the visible range. As we discussed earlier, Mn-doped CsPbCl<sub>3</sub> NCs can efficiently convert absorbed UV light into the visible range by emitting at ~600 nm with high EQE. This energy down conversion process from the NC layer can significantly reduce the parasitic absorption by substrates (*e.g.*, glass, TiO<sub>2</sub>), and thus boost the overall PCE of such devices. In addition, UV light is considered the major factor leading to destabilization of PSCs due to the photocatalytic decomposition of HP bulk thin films caused by TiO<sub>2</sub>.<sup>96</sup> In this work, the reduction of UV light significantly enhanced the stability of PSCs as illustrated in Fig. 7e. In another approach, Chen *et al.* incorporated a layer of self-assembled CsPbBr<sub>3</sub> nanowires on top of a MAPbI<sub>3</sub> HP bulk thin film, which could recycle unabsorbed photons through a fluorescence resonance energy transfer process back to the bulk thin film absorber layer.<sup>188</sup> They claimed that CsPbBr<sub>3</sub> NWs here served as the localized “gratings” for the photon management, which were responsible for the enhancement of PCE by 13% compared with the NC-free case. Luminescent solar concentrators (LSCs) are optoelectronic devices that concentrate sunlight to a small area, therefore reducing the area of solar cell devices while maintaining high power output.<sup>189–191</sup> The Mn-doped CsPbCl<sub>3</sub> NCs have been used to fabricate large area LSCs.<sup>123</sup> The large Stokes shift for Mn dopant PL, as discussed above, almost eliminates reabsorption in the LSC. Together with recent advance on high-irradiance tolerant PSC, Such HP NCs LSCs have great potential as low-cost solution in large scale PV applications.<sup>192</sup>

## 5. HP NC-Assembled Thin-Film PSCs

The other way of incorporating HP NCs in PSCs is to assemble them into NC thin film structures to serve as light absorber layers. Compared with their HP bulk counterparts, the HP NC-assembled thin films offer unique merits. They often exhibit a high  $V_{OC}$  compared with bulk thin-film PSC made with the same composition.<sup>57</sup> Other important merits include the stabilization of metastable HP phases by microstrain and the feasibility of making bilayer HP thin film structures, which will be discussed below.

The first demonstration of HP NC-assembled thin film PSCs was reported by Swarnkar *et al.* in 2016, where they achieved highly stable and efficient PSCs using CsPbI<sub>3</sub> HP NC-assembled thin films.<sup>57</sup> From the material aspect, there has been a high interest in CsPbI<sub>3</sub> HP for PSC applications due to its superior thermal stability compared with the hybrid organic-inorganic counterparts and its bandgap around 1.7 eV that is ideal for tandem PV applications. However, CsPbI<sub>3</sub> HP can easily transform to a non-perovskite orthorhombic phase in ambient conditions, which has been a major hurdle that holds back the development of CsPbI<sub>3</sub> PSCs. In this regard, significant efforts have been devoted in developing ways to stabilize CsPbI<sub>3</sub> HPs.<sup>193–196</sup> In the study by Swarnkar *et al.*, a new fabrication method of CsPbI<sub>3</sub> HP thin films was reported based on a layer-by-layer assembly of CsPbI<sub>3</sub> HP NCs together with an effective

ligand removal process using methyl acetate (Fig. 8a,b).<sup>57</sup> The CsPbI<sub>3</sub> HP NCs were found to remain in the NC form after the thin film fabrication. They claimed that the lattice strain of the NCs was an important factor that stabilized the cubic phase of CsPbI<sub>3</sub> HP NCs, preventing them from transforming into the non-perovskite orthorhombic phase.<sup>57</sup> The resultant PSC device showed a high PCE of 10.77 % with a very impressive  $V_{OC}$  of 1.23V for CsPbI<sub>3</sub> PSCs. However, this PSC showed relatively low  $J_{SC}$ , suggesting that the electronic coupling between NCs is the PSC performance bottleneck for this structure. Potential reasons that were responsible for the poor electronic coupling could be due to the presence of capping ligands causing high electric resistance. In order to overcome this issue, in a following study reported by the same group, thin layers of halide salts (*e.g.*, FAI, MAI, CsI) were solution-coated on individual NCs in the CsPbI<sub>3</sub> NC-assembled HP NC thin films.<sup>197</sup> This technique greatly enhanced the electronic coupling between NCs, as shown by a significantly increased  $J_{SC}$  from 9.22 to 14.37 mA/cm<sup>2</sup> (Fig. 8c).<sup>197</sup> In a very recent work, the ligand-removal mechanism using esters was studied by the same group.<sup>198</sup> The *in situ* hydrolysis of methyl acetate was shown to be of great importance. By controlling the humidity and treatment time, oleic acid and oleylamine were effectively replaced by formamidinium and acetate. The film-based ligand exchange from bulky ligands (*i.e.*, oleic acid, oleylamine) to short ligands resulted in a surprisingly high  $J_{OC}$  (15.4 mA/cm<sup>2</sup>) for HP NC PSCs. The weak NCs electronic coupling in HP NC-assembled thin films can be also mitigated by using highly conductive materials, such as carbon nanomaterials as 3D scaffolds to support the NC-assembled HP thin films. Wang *et al.* employed  $\mu$ -graphene to crosslink CsPbI<sub>3</sub> NCs and formed a thin film with much improved carrier transport characteristics.<sup>199</sup> After the  $\mu$ -graphene integration, the overall PCE of the PSCs using CsPbI<sub>3</sub> NC-assembled thin films was increased from 10.41% to 11.40%. Meanwhile, the  $\mu$ -graphene integration offered additional merits by enhancing the film stability under moisture and thermal stresses, providing a high device stability.

Compared with the I-based counterpart, CsPbBr<sub>3</sub> HPs exhibit enhanced moisture tolerance and phase stability due to their more ideal tolerance factor of the perovskite structure and stronger Pb-X bonds.<sup>200</sup> In spite of their relatively low PCE due to the intrinsically high bandgap (2.3 eV), CsPbBr<sub>3</sub> PSCs can potentially deliver a higher  $V_{OC}$ . Akkerman *et al.* reported a fast, room-temperature synthesis of a high-concentration ink containing CsPbBr<sub>3</sub> HP NCs capped by short, low-boiling-point ligands.<sup>70</sup> This ink was used directly for making the NC-assembled HP thin films with no requirement of lengthy post-synthetic treatments. PSCs constructed using this ink, showed a  $V_{OC}$  as high as 1.5 V and  $J_{OC}$  of 5.7 mA/cm<sup>2</sup>. In another study by Palazon *et al.*, CsPbBr<sub>3</sub> HP NC-assembled thin films were first fabricated, followed by a post treatment using thiocyanate dissolved in an ethyl acetate (EA) solution. The EA solution can efficiently remove ligands, and convert the NC thin film into a compact CsPbBr<sub>3</sub> bulk thin film.<sup>131</sup> This method addressed challenges in preparing high-quality CsPbBr<sub>3</sub> HP bulk thin films by using HP NCs as ‘precursors’, at moderate

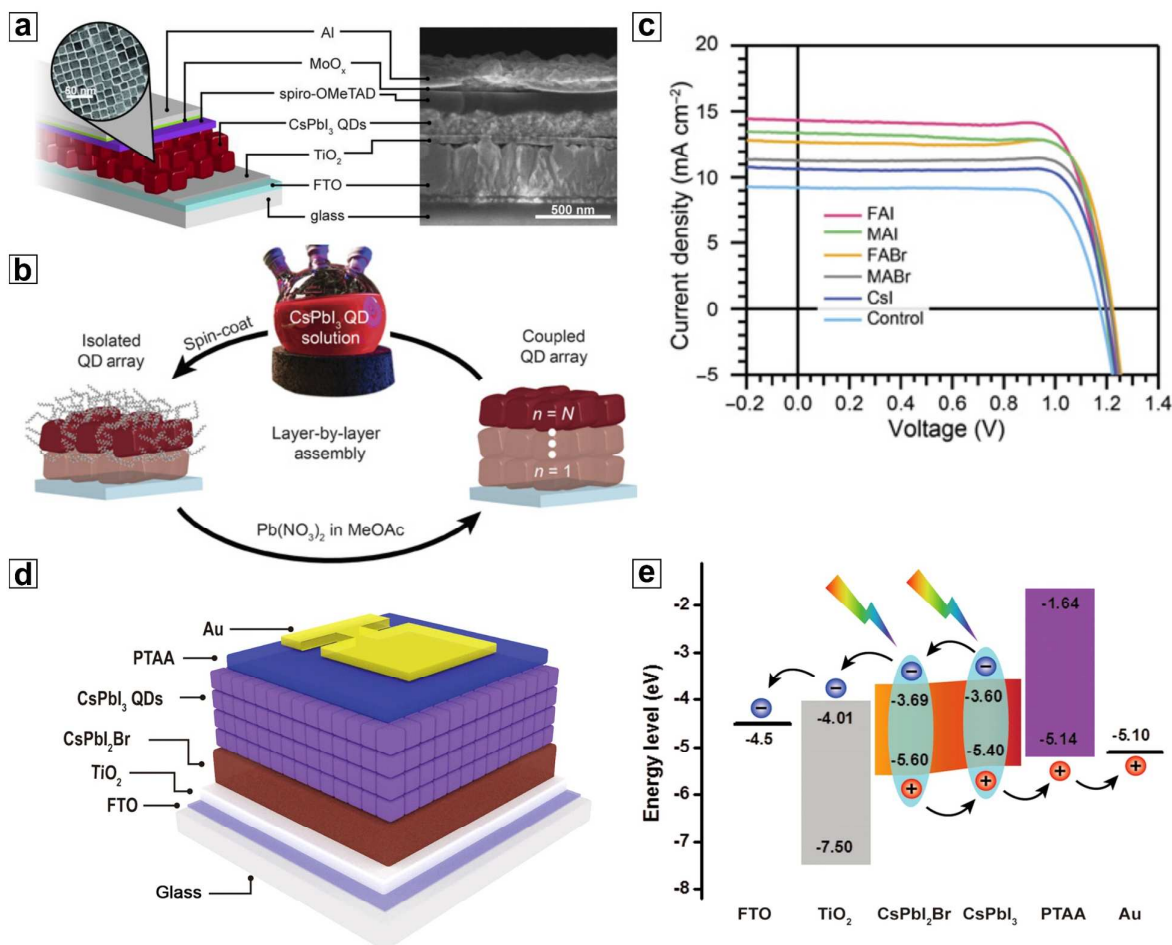


**Figure 8.** (a) Schematic representation of the device structure and the cross section scanning electron microscope (SEM) image of the PSC based on a CsPbI<sub>3</sub> NCs-assembled thin film. (b) Schematic of the film deposition and post-treatment procedure. (c) Current-density-voltage scan of the device treated with different salt additives. (d) Schematic illustration of the graded bandgap PSC made using a bilayer of a CsPbI<sub>2</sub>Br HP bulk thin film and a CsPbI<sub>3</sub> HP NCs-assembled thin film. (e) Energy level diagram for the device in (d). (a) is reproduced from ref. 57 with permission of American Association for the Advancement of Science. (b,c) are reproduced from ref. 197 with permission of American Association for the Advancement of Science. (d,e) are reproduced from ref. 201 with permission of Elsevier

temperatures. It was found that by using this method, a small amount of CsPb<sub>2</sub>Br<sub>5</sub> phase well-dispersed within the final CsPbBr<sub>3</sub> HP thin film, leading to an interesting reduction in trap density. As a result, the CsPbBr<sub>3</sub> PSC showed a PCE of 6.81%, which is higher than that of CsPbBr<sub>3</sub> PSCs made by conventional methods.

Tandem solar cell design is an important method to push device PCE beyond the Shockley-Queisser limit.<sup>105</sup> To this end, HP NC-assembled thin films can serve as one absorbing layer combined with another layer of either HP bulk thin films or HP NCs with a complementary bandgap gradient. This is primarily attributed to the capability of depositing NC-assembled thin films using solvents which do not interact with the existing HP bulk thin films. Very recently, Bian *et al.* reported a proof-of-concept demonstration in this regard.<sup>201</sup> In their study, they first fabricated a CsPbI<sub>2</sub>Br HP bulk thin film with a 1.91 eV bandgap as the main absorber. Afterwards, a CsPbI<sub>3</sub> NC-assembled HP thin film with a bandgap of 1.77 eV was

deposited. By applying multiple strategies, including Mn cation substitution, thiocyanate capping, and FA treatment, the chemical stability and carrier mobility in the thin film could be greatly improved.<sup>201</sup> Finally, a component-graded heterojunction was formed at the CsPbI<sub>2</sub>Br-CsPbI<sub>3</sub> NC interface, leading to a favourable energy alignment for carrier collection as discussed earlier (Fig. 8c,d). This bilayer HP thin film with a gradient bandgap showed effective overall light harvesting and a PCE of 14.45% in the final device, setting a record for purely inorganic PSCs at the time.

## 6. Perspectives

Development of colloidal HP NCs and their application in PSC devices have both seen rapidly growing interest. Only four years following the first synthesis of HP NCs, numerous additional discoveries have been witnessed in the community. However, these exciting discoveries have overshadowed some fundamental challenges and difficulties that need a significant

amount of research efforts to overcome. Therefore, in this section, we would like to provide our perspectives from both the material production and the device fabrication points of view and delineate some challenges with the potential for future directions in this fascinating research field.

### Perspectives in HP NC materials

Pb-containment is one obvious problem for state-of-the-art HP NCs. Pb, as a poisonous heavy-metal element, has been under health and environmental regulations in many countries and regions. As a result, the development of Pb-free HP NCs is in pressing need. Although currently ongoing, the progress of Pb-free perovskite development has still been incomparable to the development of their Pb-based counterparts. Very recently, exemplified by the  $\text{Cs}_2\text{AgBiX}_6$  double perovskite, and the  $\text{Cs}_3\text{Sb}_2\text{X}_9$  and  $\text{MA}_3\text{Bi}_2\text{X}_9$  2D perovskites, Bi and Sb-based HP NCs have shown a number of promising properties including optical properties<sup>72</sup>, high NC stability<sup>202</sup> and controllable bandgaps.<sup>203</sup> Success in the introduction of Bi and Sb into HP NCs show an exciting future. However, other possible elements, such as Ge, Sn, Ti and In, that could also totally replace Pb while maintaining suitable optoelectronic properties, should not be neglected and additionally need to draw more research attention.

While the ion exchange reactions offer facile routes toward generation of the HP NCs with mixed anion compositions, the HP NCs with mixed cations have been studied to a much less content. In order to maximize the entropic stabilization effect, synthetic methods to achieve uniform cation alloy via either direct synthesis or cation exchange need to be further developed with a greater detail. Additionally, compared with their film counterparts, the physical and chemical properties of alloy HP NCs are less studied and understood. Photoinduced dealloying has been identified as a crucial source of degradation in alloy PSC film.<sup>204</sup> Whether nano-sized confinement and surface ligands of HP NCs can provide sufficient energy barriers that are able to suppress dealloying processes is an interesting topic to explore.

Overcoating shell materials with different band energy alignments relative to the core QD NC is a major and fruitful research area in the conventional QD NC field. Inorganic shelling has been proven to be one of the most efficient ways to manipulate, modify, and improve the chemical, physical, and optical properties of QD NCs.<sup>60,205,206</sup> Unfortunately, overcoating the HP NCs has proven to be a great challenge and has yet to be systematically studied and reliably developed. The material instability and ionic chemical nature of the HP NCs are responsible for the remaining hurdle that diminishes their applicability in conventional epitaxial core-shell growth conditions. Novel shell growth strategies under suitable conditions, such as room temperature solution-based atomic layer deposition, or non-epitaxial shell deposition, need to be specifically designed for this special category of NCs.

Capping ligands play a critically important role in both stabilizing the HP NCs in solution or solids, and in their performances following device fabrications. The low current density and large hysteresis in NC solar cells are largely attributed to the presence of insulating long, organic ligands. A rationally designed ligand system could be the key to solve these problems. Current studies on fabricating NC-based PSCs mostly rely on complete removal of the long organic ligands using an antisolvent purification procedure. Such a process, however, can cause damage to the integrity of the HP NCs. Therefore, novel methods for ligand removal during the PSC fabrication need to be developed. In another approach, before solidified into films, HP NCs can be equipped with novel-designed ligands through solution phase ligand exchanges. The HP NCs with device-compatible ligands could then be directly applied in subsequent thin film fabrication without any additional tedious ligand removal processes. In traditional QD-based solar cells, inorganic ligands, such as thiocyanate or metal chalcogenide complexes started to be used in recent years to reduce the inter-particle distances with minimal impacts on NC film morphology.<sup>207</sup> These inorganic molecules, with small size and ionic form, are integratable in PV devices, and should also be considered as a potential ligand set for HP NCs. In addition, the NC printing technique requires highly concentrated NC inks with superior particle stability and dispersity. Recent studies have demonstrated that the solubility of NCs relies on not only the chain length of ligands, but also their molecular structure.<sup>208</sup> Therefore, modulating the interparticle interactions through ligands may be the key to achieve ideal NC inks with high concentrations and suitable chemical and physical properties.

Thinking in advance, when aiming towards production and commercialization of the HP NC-based PSCs, HP NC synthesis at a large-scale is unavoidable. Both LARP and hot-injection procedures rely on rapid precursor injection and fast mass transport to reach an instantaneous nucleation followed by NC growth. Although possible, both methods are not ideal for scaling up to an industrial level at low cost. Therefore, more inert and low-cost precursors that can be applied to easy-to-

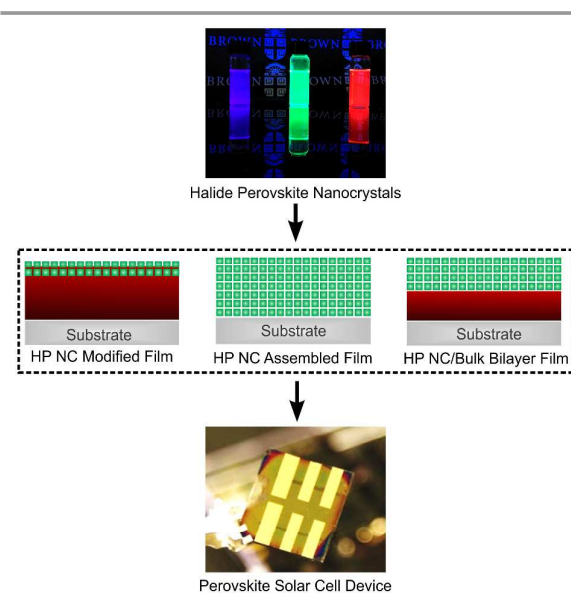


**Figure 2.** Schematic diagram for the fabrication techniques from perovskite NC to PSC.

scale-up methods, such as a non-injection heating up procedure,<sup>209,210</sup> together with novel reactor designs could serve as a research direction that needs more development along the way.

Taking advantage of their intrinsic material nature along with more than three decades of NC synthetic method development, HP NCs have been synthesized almost instantly with high sample uniformity. This high morphological uniformity allows for easy fabrications of HP NC superstructures from individual building blocks through self-assembly strategies. In particular, large-area HP NC superlattice thin films with a well-ordered particle close-packing possess a higher packing density and smoother film morphology than randomly packed ones. The superlattice thin film may show enhanced optoelectronic properties for PSC applications. In addition, the atomic alignments through orientated attachment,<sup>211,212</sup> and NC substitutional doping in superlattices,<sup>213</sup> have recently proven to be important to dramatically enhance charge transfer and thus improve the electronic properties of QD NC superlattice thin films. These tricks should be easily transferred to the HP NC superlattice systems. Furthermore, given the flexibility in the selection of NC building blocks, HP NCs with different size, shape and compositions, or even mixed with other NC types, in principle can be used for construction of the HP NC superstructures with unprecedented complexities. Multi-layer tandem PSCs with highly customized and designed band energy alignments, otherwise inaccessible through HP bulk materials, become feasible. All of these studies are currently lacking in the field. Exciting discoveries should be anticipated.

#### Perspectives in integration of HP NCs in PSCs

Rich interactions of HP NCs with light offer them great potential to be applied in optoelectronic devices. Despite their superior intrinsic properties as we discussed, HP NCs need to be efficiently integrated into PSC devices with well-customized designs. As shown in Fig. 9, HP NCs can be applied into PSCs as one of the following three components: (i) the modifiers/additives for HP bulk thin films, (ii) the sole building blocks of NC thin film light-absorbers, or (iii) the added building blocks for making graded bandgap PSCs. While some research has been done in these directions as summarized above, there is still large room to explore with the potential to build PSCs with performances beyond that of the state-of-the-art devices.

For the use of HP NCs as modifiers, the following research directions may emerge. First, the current research has been limited to enhancing the surfaces/interfaces of the bulk HP thin films in PSCs. In fact, grain boundaries in HP bulk thin films are one of the most prominent microstructures that play a vital role on the PV performance and device stability. The congeneric nature of HP NCs allows for the modification of bulk thin film grain boundaries at minimal cost. The defects at grain boundaries can be passivated and the band diagram may be tuned in our favour. Additionally, the HP NC-modified grain

boundary could even be possibly endowed with new optical/electronic functions. Second, as discussed, the wide tunability in morphology and composition makes HP NCs ideal 'seed' materials for solution crystallization of HP bulk thin films. Nanocubes, nanosheets, nanowires and their ordered self-assemblies can be synthesized. They can then be introduced in the HP thin film crystallization process as heterogenous nucleation sites. These pre-engineered NC "seeds" may help guide the HP crystallization in a controllable manner resulting in precise control over the final thin film microstructures. Nevertheless, this is still challenging considering the sensitivity of HP NCs in the perovskite precursor solutions. Such difficulty may be lifted through ligand-engineering of the HP NCs using ionic ligands or through the synthesis of polar-solvent-tolerant NCs. Third, HP NCs can also serve as dopants in the HP bulk thin films. Through innovative deposition strategies, HP NCs may be deliberately incorporated at certain locations in the bulk thin films, enabling site-specific doping. This position-controlled HP NC doping may improve the electronic properties of the HP bulk thin films, and thus the performance of the resultant PSCs.

For the use of HP NCs as the sole building blocks of the light absorber layer in PSCs, immense opportunities remain for further investigation in this direction. First, the state-of-the-art fabrication methods of HP NC-assembled thin films are generally very tedious and are not suitable for the commercial PSC production. The bottleneck for the processing of NC-assembled thin films is the necessity of repeated deposition and ligand-washing steps, which is mainly due to the relatively low concentration of the NCs inks and the unfavourable long organic ligands. By using high-concentration NC inks with short inorganic ligands as discussed earlier, the fabrication procedure can be dramatically simplified. Very recently, highly efficient LEDs were fabricated using FAPbBr<sub>3</sub> NC film that was synthesized by an *in situ* LARP process during spin-coating.<sup>214</sup> This study may inspire new strategies for HP NC thin film fabrication in PSCs. In addition to the spin-coating method, many scalable deposition protocols, such as spray-coating, doctor-blading, and slot-die coating, may be applied for making HP NC-assembled thin films. This represents a completely new research paradigm. Second, the as-studied HP NCs-assembled thin films and PSCs have previously only focused on using the all-inorganic HP compositions, such as CsPbI<sub>3</sub> and CsPbBr<sub>3</sub>. These compositions exhibit bandgaps that are too large for the operation of single-junction solar cells. Therefore, lower-band-gap HP-NC-assembled thin films need to be prepared for improving the PCE of PSCs. For example, FAPbI<sub>3</sub> HPs show a much smaller bandgap than CsPbI<sub>3</sub> HPs and exhibit a similar perovskite-to-non-perovskite phase transition behaviour as CsPbI<sub>3</sub> HP in ambient conditions. It would be interesting to see whether the NC-induced phase stabilization also applies and whether improved PCE and stability can be simultaneously achieved in the FAPbI<sub>3</sub> NC-assembled thin film PSCs. In addition, HP NCs may also enable the fabrication of other thin films with compositions unstable in their bulk phases (*e.g.*, Cs<sub>2</sub>AgBiI<sub>6</sub>), which can be particularly important for

developing novel Pb-free PSCs. Third, as discussed already, the electronic coupling between HP NCs is of vital importance for good charge transport dynamics in HP NCs-assembled superlattice thin films. While it has been demonstrated that overcoating NCs with suitable shell materials is a viable method for enhancing the electronic coupling of HP-NC-films,<sup>197</sup> it may be feasible to use core-shell structured HP NCs for a direct assembly of HP NC superstructured thin films with a high charge mobility.

Ability to serve as the building blocks for making graded-bandgap PSCs is one of the most unique features of HP NCs. This is mainly owing to the orthogonal solvents for the deposition of HP NCs and HP bulk thin films. While the proof-of-concept study of a graded-bandgap CsPb<sub>2+x</sub>Br<sub>1-x</sub> PSC has been demonstrated<sup>186</sup>, the optical bandgaps and film structures in this reported PSC device are far from being optimized. Continued research in this direction offers vast opportunities for generating PSCs with PCEs approaching the Shockley-Queisser limit.

### Concluding Remarks

The rapid development of HP materials brings exciting ideas and encouraging applications in the field of optoelectronics. The recently developed synthetic approaches for monodispersed HP NCs enabled in-depth studies of these materials for potential PSC applications. The use of HP NCs in PSC applications takes advantage of their tunable electronic properties, their well-defined crystal domains, and their crystal structural and compositional similarities to bulk HP materials. HP NCs have shown promising results both as thin film modifiers, and as light absorbers in PSC devices. We believe that this perspective article can not only provide insights into the as-made discoveries, but more importantly delineate some future directions toward bridging HP NCs tightly with PSCs. To further advance this fascinating research direction, improvements on NC stability and surface ligand states is highly desirable. With a library of HP NC building blocks and newly developed synthetic tools, novel PSC structures and PV fabrication techniques with the integration of HP NCs are likely to emerge.

### Conflicts of interest

The authors declare no conflict of interest.

### Acknowledgements

Y. Zhang, Y. Zhou and O. Chen acknowledge the support from the National Science Foundation (OIA-1538893) and Brown University's Institute for Molecular and Nanoscale Innovation Seed Program. Y. Zhou. and Y. Zhang also acknowledge Prof. N.P. Padture at Brown University for the insightful discussion and the generous support. H. Yang and O. Chen acknowledge the support from the Brown University startup fund. K. Hills-

Kimball is supported by the US Department of Education, GAANN Award (P200A150037).

### Notes and references

- 1 D. Weber, *Zeitschrift für Naturforsch. B*, 1978, **33**, 1443–1445.
- 2 W. H. L., *Zeitschrift für Anorg. Chemie*, 1893, **3**, 195–210.
- 3 C. H. R. K. N. MØLLER, *Nature*, 1958, **182**, 1436.
- 4 C. C. Stoumpos, C. D. Malliakas and M. G. Kanatzidis, *Inorg. Chem.*, 2013, **52**, 9019–9038.
- 5 I. Chung, J. H. Song, J. Im, J. Androulakis, C. D. Malliakas, H. Li, A. J. Freeman, J. T. Kenney and M. G. Kanatzidis, *J. Am. Chem. Soc.*, 2012, **134**, 8579–8587.
- 6 C. C. Stoumpos, L. Frazer, D. J. Clark, Y. S. Kim, S. H. Rhim, A. J. Freeman, J. B. Ketterson, J. I. Jang and M. G. Kanatzidis, *J. Am. Chem. Soc.*, 2015, **137**, 6804–6819.
- 7 J. Calabrese, N. L. Jones, R. L. Harlow, N. Herron, D. L. Thorn and Y. Wang, *J. Am. Chem. Soc.*, 1991, **113**, 2328–2330.
- 8 T. Goto, H. Makino, T. Yao, C. H. Chia, T. Makino, Y. Segawa, G. A. Mousdis and G. C. Papavassiliou, *Phys. Rev. B*, 2006, **73**, 115206.
- 9 D. B. Mitzi, S. Wang, C. A. Feild, C. A. Chess and A. M. Guloy, *Science*, 1995, **267**, 1473–1476.
- 10 R. Burnus and G. Meyer, *Zeitschrift für Anorg. und Allg. Chemie*, 1991, **602**, 31–37.
- 11 B. Saparov, F. Hong, J. P. Sun, H. S. Duan, W. Meng, S. Cameron, I. G. Hill, Y. Yan and D. B. Mitzi, *Chem. Mater.*, 2015, **27**, 5622–5632.
- 12 B. Lee, C. C. Stoumpos, N. Zhou, F. Hao, C. Malliakas, C. Y. Yeh, T. J. Marks, M. G. Kanatzidis and R. P. H. Chang, *J. Am. Chem. Soc.*, 2014, **136**, 15379–15385.
- 13 M.-G. Ju, M. Chen, Y. Zhou, J. Dai, L. Ma, N. P. Padture and X. C. Zeng, *Joule*, 2018, **2**, 1231–1241.
- 14 Y. Zhou, O. S. Game, S. Pang and N. P. Padture, *J. Phys. Chem. Lett.*, 2015, **6**, 4827–4839.
- 15 M. Era, S. Morimoto, T. Tsutsui and S. Saito, *Appl. Phys. Lett.*, 1994, **65**, 676–678.
- 16 Z.-K. Tan, R. S. Moghaddam, M. L. Lai, P. Docampo, R. Higler, F. Deschler, M. Price, A. Sadhanala, L. M. Pazos, D. Credgington, F. Hanusch, T. Bein, H. J. Snaith and R. H. Friend, *Nat. Nanotechnol.*, 2014, **9**, 687–692.
- 17 G. Xing, N. Mathews, S. S. Lim, N. Yantara, X. Liu, D. Sabba, M. Grätzel, S. Mhaisalkar and T. C. Sum, *Nat. Mater.*, 2014, **13**, 476–480.
- 18 F. Deschler, M. Price, S. Pathak, L. E. Klintberg, D. D. Jarausch, R. Higler, S. Hüttner, T. Leijtens, S. D. Stranks, H. J. Snaith, M. Atatüre, R. T. Phillips and R. H. Friend, *J. Phys. Chem. Lett.*, 2014, **5**, 1421–1426.
- 19 L. Dou, Y. Yang, J. You, Z. Hong, W.-H. Chang, G. Li and Y. Yang, *Nat. Commun.*, 2014, **5**, 5404.
- 20 C. C. Stoumpos, C. D. Malliakas, J. A. Peters, Z. Liu, M. Sebastian, J. Im, T. C. Chasapis, A. C. Wibowo, D. Y. Chung, A. J. Freeman, B. W. Wessels and M. G. Kanatzidis, *Cryst. Growth Des.*, 2013, **13**, 2722–2727.
- 21 H. Zhu, Y. Fu, F. Meng, X. Wu, Z. Gong, Q. Ding, M. V.

- Gustafsson, M. T. Trinh, S. Jin and X.-Y. Zhu, *Nat. Mater.*, 2015, **14**, 636–642.
- 22 W. Pan, H. Wu, J. Luo, Z. Deng, C. Ge, C. Chen, X. Jiang, W.-J. Yin, G. Niu, L. Zhu, L. Yin, Y. Zhou, Q. Xie, X. Ke, M. Sui and J. Tang, *Nat. Photonics*, 2017, **11**, 726–732.
- 23 S. Yakunin, M. Sytnyk, D. Kriegner, S. Shrestha, M. Richter, G. J. Matt, H. Azimi, C. J. Brabec, J. Stangl, M. V. Kovalenko and W. Heiss, *Nat. Photonics*, 2015, **9**, 444–449.
- 24 H. Wei, Y. Fang, P. Mulligan, W. Chuirazzi, H.-H. Fang, C. Wang, B. R. Ecker, Y. Gao, M. A. Loi, L. Cao and J. Huang, *Nat. Photonics*, 2016, **10**, 333–339.
- 25 A. Kojima, K. Teshima, Y. Shirai and T. Miyasaka, *J. Am. Chem. Soc.*, 2009, **131**, 6050–6051.
- 26 W. S. Yang, B.-W. Park, E. H. Jung, N. J. Jeon, Y. C. Kim, D. U. Lee, S. S. Shin, J. Seo, E. K. Kim, J. H. Noh and S. Il Seok, *Science*, 2017, **356**, 1376–1379.
- 27 NREL's "Best Research-Cell Efficiencies" Chart, <https://www.nrel.gov/pv/assets/pdfs/pv-efficiencies-07-17-2018.pdf>. Accessed on August 24, 2018.
- 28 S. De Wolf, J. Holovsky, S. J. Moon, P. Löper, B. Niesen, M. Ledinsky, F. J. Haug, J. H. Yum and C. Ballif, *J. Phys. Chem. Lett.*, 2014, **5**, 1035–1039.
- 29 E. Edri, S. Kirmayer, M. Kulbak, G. Hodes and D. Cahen, *J. Phys. Chem. Lett.*, 2014, **5**, 429–433.
- 30 J. H. Noh, S. H. Im, J. H. Heo, T. N. Mandal and S. Il Seok, *Nano Lett.*, 2013, **13**, 1764–1769.
- 31 C. S. Ponceca, T. J. Savenije, M. Abdellah, K. Zheng, A. Yartsev, T. Pascher, T. Harlang, P. Chabera, T. Pullerits, A. Stepanov, J.-P. Wolf and V. Sundström, *J. Am. Chem. Soc.*, 2014, **136**, 5189–5192.
- 32 Q. Dong, Y. Fang, Y. Shao, P. Mulligan, J. Qiu, L. Cao and J. Huang, *Science*, 2015, **347**, 967–970.
- 33 J. Burschka, N. Pellet, S. J. Moon, R. Humphry-Baker, P. Gao, M. K. Nazeeruddin and M. Grätzel, *Nature*, 2013, **499**, 316–319.
- 34 D. Shi, V. Adinolfi, R. Comin, M. Yuan, E. Alarousu, A. Buin, Y. Chen, S. Hoogland, A. Rothenberger, K. Katsiev, Y. Losovyj, X. Zhang, P. A. Dowben, O. F. Mohammed, E. H. Sargent and O. M. Bakr, *Science*, 2015, **347**, 519–522.
- 35 M. Liu, M. B. Johnston and H. J. Snaith, *Nature*, 2013, **501**, 395–398.
- 36 W. Li, J. Fan, J. Li, Y. Mai and L. Wang, *J. Am. Chem. Soc.*, 2015, **137**, 10399–10405.
- 37 Y. Zhou, M. Yang, W. Wu, A. L. Vasiliev, K. Zhu and N. P. Padture, *J. Mater. Chem. A*, 2015, **3**, 8178–8184.
- 38 M. M. Lee, J. Teuscher, T. Miyasaka, T. N. Murakami and H. J. Snaith, *Science*, 2012, **338**, 643–647.
- 39 P. Docampo, J. M. Ball, M. Darwich, G. E. Eperon and H. J. Snaith, *Nat. Commun.*, 2013, **4**, 1–6.
- 40 C. D. Bailie, M. G. Christoforo, J. P. Mailoa, A. R. Bowring, E. L. Unger, W. H. Nguyen, J. Burschka, N. Pellet, J. Z. Lee, M. Grätzel, R. Noufi, T. Buonassisi, A. Salleo and M. D. McGehee, *Energy Environ. Sci.*, 2015, **8**, 956–963.
- 41 H. Huang, A. S. Sussha, S. V. Kershaw, T. F. Hung and A. L. Rogach, *Adv. Sci.*, 2015, **2**, 1500194.
- 42 F. Liu, Y. Zhang, C. Ding, S. Kobayashi, T. Izuishi, N. Nakazawa, T. Toyoda, T. Ohta, S. Hayase, T. Minemoto, K. Yoshino, S. Dai and Q. Shen, *ACS Nano*, 2017, **11**, 10373–10383.
- 43 G. Nedelcu, L. Protesescu, S. Yakunin, M. I. Bodnarchuk, M. J. Grotevent and M. V. Kovalenko, *Nano Lett.*, 2015, **15**, 5635–5640.
- 44 Q. A. Akkerman, V. D'Innocenzo, S. Accornero, A. Scarpellini, A. Petrozza, M. Prato and L. Manna, *J. Am. Chem. Soc.*, 2015, **137**, 10276–10281.
- 45 F. Palazon, F. Di Stasio, S. Lauciello, R. Krahne, M. Prato and L. Manna, *J. Mater. Chem. C*, 2016, **4**, 9179–9182.
- 46 W. van der Stam, J. J. Geuchies, T. Altantzis, K. H. W. van den Bos, J. D. Meeldijk, S. Van Aert, S. Bals, D. Vanmaekelbergh and C. de Mello Donega, *J. Am. Chem. Soc.*, 2017, **139**, 4087–4097.
- 47 Z. Liu, Y. Bekenstein, X. Ye, S. C. Nguyen, J. Swabeck, D. Zhang, S.-T. Lee, P. Yang, W. Ma and A. P. Alivisatos, *J. Am. Chem. Soc.*, 2017, **139**, 5309–5312.
- 48 B. Wang, C. Zhang, S. Huang, Z. Li, L. Kong, L. Jin, J. Wang, K. Wu and L. Li, *ACS Appl. Mater. Interfaces*, 2018, **10**, 23303–23310.
- 49 J. Song, J. Li, X. Li, L. Xu, Y. Dong and H. Zeng, *Adv. Mater.*, 2015, **27**, 7162–7167.
- 50 Z. Shi, Y. Li, Y. Zhang, Y. Chen, X. Li, D. Wu, T. Xu, C. Shan and G. Du, *Nano Lett.*, 2017, **17**, 313–321.
- 51 H. Cho, S.-H. Jeong, M.-H. Park, Y.-H. Kim, C. Wolf, C.-L. Lee, J. H. Heo, A. Sadhanala, N. Myoung, S. Yoo, S. H. Im, R. H. Friend and T.-W. Lee, *Science*, 2015, **350**, 1222–1225.
- 52 F. Krieg, S. T. Ochsenein, S. Yakunin, S. ten Brinck, P. Aellen, A. Süess, B. Clerc, D. Guggisberg, O. Nazarenko, Y. Shynkarenko, S. Kumar, C.-J. Shih, I. Infante and M. V. Kovalenko, *ACS Energy Lett.*, 2018, **3**, 641–646.
- 53 J. Kang and L.-W. Wang, *J. Phys. Chem. Lett.*, 2017, **8**, 489–493.
- 54 M. Lorenzon, L. Sortino, Q. Akkerman, S. Accornero, J. Pedrini, M. Prato, V. Pinchetti, F. Meinardi, L. Manna and S. Brovelli, *Nano Lett.*, 2017, **17**, 3844–3853.
- 55 Y. Dong, T. Qiao, D. Kim, D. Parobek, D. Rossi and D. H. Son, *Nano Lett.*, 2018, **18**, 3716–3722.
- 56 L. Protesescu, S. Yakunin, M. I. Bodnarchuk, F. Bertolotti, N. Masciocchi, A. Guagliardi and M. V. Kovalenko, *J. Am. Chem. Soc.*, 2016, **138**, 14202–14205.
- 57 A. Swarnkar, A. R. Marshall, E. M. Sanehira, B. D. Chernomordik, D. T. Moore, J. A. Christians, T. Chakrabarti and J. M. Luther, *Science*, 2016, **354**, 92–95.
- 58 M. Cha, P. Da, J. Wang, W. Wang, Z. Chen, F. Xiu, G. Zheng and Z.-S. Wang, *J. Am. Chem. Soc.*, 2016, **138**, 8581–8587.
- 59 C. B. Murray, D. J. Norris and M. G. Bawendi, *J. Am. Chem. Soc.*, 1993, **115**, 8706–8715.
- 60 O. Chen, H. Wei, A. Maurice, M. Bawendi and P. Reiss, *MRS Bull.*, 2013, **38**, 696–702.
- 61 R. Plass, S. Pelet, J. Krueger, M. Grätzel and U. Bach, *J. Phys. Chem. B*, 2002, **106**, 7578–7580.
- 62 K. Barnham, J. L. Marques, J. Hassard and P. O'Brien, *Appl. Phys. Lett.*, 2000, **76**, 1197–1199.
- 63 S. Fig, *Nature*, 2002, **420**, 3–6.
- 64 I. L. Medintz, H. T. Uyeda, E. R. Goldman and H. Mattoussi, *Nat. Mater.*, 2005, **4**, 435–446.

- 65 L. C. Schmidt, A. Pertegás, S. González-Carrero, O. Malinkiewicz, S. Agouram, G. Mínguez Espallargas, H. J. Bolink, R. E. Galian and J. Pérez-Prieto, *J. Am. Chem. Soc.*, 2014, **136**, 850–853.
- 66 F. Zhang, H. Zhong, C. Chen, X. Wu, X. Hu, H. Huang, J. Han, B. Zou and Y. Dong, *ACS Nano*, 2015, **9**, 4533–4542.
- 67 S. Sun, D. Yuan, Y. Xu, A. Wang and Z. Deng, *ACS Nano*, 2016, **10**, 3648–3657.
- 68 M. C. Weidman, M. Seitz, S. D. Stranks and W. A. Tisdale, *ACS Nano*, 2016, **10**, 7830–7839.
- 69 S. Bhaumik, S. A. Veldhuis, Y. F. Ng, M. Li, S. K. Muduli, T. C. Sum, B. Damodaran, S. Mhaisalkar and N. Mathews, *Chem. Commun.*, 2016, **52**, 7118–7121.
- 70 Q. A. Akkerman, M. Gandini, F. Di Stasio, P. Rastogi, F. Palazon, G. Bertoni, J. M. Ball, M. Prato, A. Petrozza and L. Manna, *Nat. Energy*, 2016, **2**, 16194.
- 71 M. Leng, Z. Chen, Y. Yang, Z. Li, K. Zeng, K. Li, G. Niu, Y. He, Q. Zhou and J. Tang, *Angew. Chemie Int. Ed.*, 2016, **55**, 15012–15016.
- 72 J. Zhang, Y. Yang, H. Deng, U. Farooq, X. Yang, J. Khan, J. Tang and H. Song, *ACS Nano*, 2017, **11**, 9294–9302.
- 73 F. Zhang, S. Huang, P. Wang, X. Chen, S. Zhao, Y. Dong and H. Zhong, *Chem. Mater.*, 2017, **29**, 3793–3799.
- 74 L. Protesescu, S. Yakunin, M. I. Bodnarchuk, F. Krieg, R. Caputo, C. H. Hendon, R. X. Yang, A. Walsh and M. V. Kovalenko, *Nano Lett.*, 2015, **15**, 3692–3696.
- 75 G. Almeida, L. Goldoni, Q. Akkerman, Z. Dang, A. H. Khan, S. Marras, I. Moreels and L. Manna, *ACS Nano*, 2018, **12**, 1704–1711.
- 76 M. Imran, V. Caligiuri, M. Wang, L. Goldoni, M. Prato, R. Krahne, L. De Trizio and L. Manna, *J. Am. Chem. Soc.*, 2018, **140**, 2656–2664.
- 77 Y. Bekenstein, B. A. Koscher, S. W. Eaton, P. Yang and A. P. Alivisatos, *J. Am. Chem. Soc.*, 2015, **137**, 16008–16011.
- 78 Q. A. Akkerman, S. G. Motti, A. R. Srimath Kandada, E. Mosconi, V. D’Innocenzo, G. Bertoni, S. Marras, B. A. Kamino, L. Miranda, F. De Angelis, A. Petrozza, M. Prato and L. Manna, *J. Am. Chem. Soc.*, 2016, **138**, 1010–1016.
- 79 M. Imran, F. Di Stasio, Z. Dang, C. Canale, A. H. Khan, J. Shamsi, R. Brescia, M. Prato and L. Manna, *Chem. Mater.*, 2016, **28**, 6450–6454.
- 80 X. Sheng, G. Chen, C. Wang, W. Wang, J. Hui, Q. Zhang, K. Yu, W. Wei, M. Yi, M. Zhang, Y. Deng, P. Wang, X. Xu, Z. Dai, J. Bao and X. Wang, *Adv. Funct. Mater.*, 2018, **3**, 1800283.
- 81 Z.-J. Li, E. Hofman, A. H. Davis, M. M. Maye and W. Zheng, *Chem. Mater.*, 2018, **30**, 3854–3860.
- 82 D. Zhang, S. W. Eaton, Y. Yu, L. Dou and P. Yang, *J. Am. Chem. Soc.*, 2015, **137**, 9230–9233.
- 83 M. V. Kovalenko and M. I. Bodnarchuk, *Chim. Int. J. Chem.*, 2017, **71**, 461–470.
- 84 K.-H. Wang, J.-N. Yang, Q.-K. Ni, H.-B. Yao and S.-H. Yu, *Langmuir*, 2018, **34**, 595–602.
- 85 Y. Tong, E.-P. Yao, A. Manzi, E. Bladt, K. Wang, M. Döblinger, S. Bals, P. Müller-Buschbaum, A. S. Urban, L. Polavarapu and J. Feldmann, *Adv. Mater.*, 2018, **30**, 1801117.
- 86 L. Protesescu, S. Yakunin, S. Kumar, J. B?r, F. Bertolotti, N. Masciocchi, A. Guagliardi, M. Grotevent, I. Shorubalko, M. I. Bodnarchuk, C.-J. Shih and M. V. Kovalenko, *ACS Nano*, 2017, **11**, 3119–3134.
- 87 W. Zhai, J. Lin, Q. Li, K. Zheng, Y. Huang, Y. Yao, X. He, L. Li, C. Yu, C. Liu, Y. Fang, Z. Liu and C. Tang, *Chem. Mater.*, 2018, **30**, 3714–3721.
- 88 M. Chen, Y. Zou, L. Wu, Q. Pan, D. Yang, H. Hu, Y. Tan, Q. Zhong, Y. Xu, H. Liu, B. Sun and Q. Zhang, *Adv. Funct. Mater.*, 2017, **27**, 1701121.
- 89 Z.-Y. Zhu, Q.-Q. Yang, L.-F. Gao, L. Zhang, A.-Y. Shi, C.-L. Sun, Q. Wang and H.-L. Zhang, *J. Phys. Chem. Lett.*, 2017, **8**, 1610–1614.
- 90 S. Yun, A. Kirakosyan, S.-G. Yoon and J. Choi, *ACS Sustain. Chem. Eng.*, 2018, **6**, 3733–3738.
- 91 L. Protesescu, S. Yakunin, O. Nazarenko, D. N. Dirin and M. V. Kovalenko, *ACS Appl. Nano Mater.*, 2018, **1**, 1300–1308.
- 92 D. M. Jang, D. H. Kim, K. Park, J. Park, J. W. Lee and J. K. Song, *J. Mater. Chem. C*, 2016, **4**, 10625–10629.
- 93 J. Almutlaq, J. Yin, O. F. Mohammed and O. M. Bakr, *J. Phys. Chem. Lett.*, 2018, **9**, 4131–4138.
- 94 J. S. Bechtel and A. Van der Ven, *Phys. Rev. Mater.*, 2018, **2**, 045401.
- 95 S. Yang, W. Fu, Z. Zhang, H. Chen and C.-Z. Li, *J. Mater. Chem. A*, 2017, **5**, 11462–11482.
- 96 M. I. Asghar, J. Zhang, H. Wang and P. D. Lund, *Renew. Sustain. Energy Rev.*, 2017, **77**, 131–146.
- 97 K. Chen, X. Deng, G. Dodekatos and H. Tüysüz, *J. Am. Chem. Soc.*, 2017, **139**, 12267–12273.
- 98 S. Huang, Z. Li, L. Kong, N. Zhu, A. Shan and L. Li, *J. Am. Chem. Soc.*, 2016, **138**, 5749–5752.
- 99 X. Di, Z. Hu, J. Jiang, M. He, L. Zhou, W. Xiang and X. Liang, *Chem. Commun.*, 2017, **53**, 11068–11071.
- 100 F. Di Stasio, S. Christodoulou, N. Huo and G. Konstantatos, *Chem. Mater.*, 2017, **29**, 7663–7667.
- 101 J. Y. Woo, Y. Kim, J. Bae, T. G. Kim, J. W. Kim, D. C. Lee and S. Jeong, *Chem. Mater.*, 2017, **29**, 7088–7092.
- 102 V. M. Goldschmidt, *Naturwissenschaften*, 1926, **14**, 477–485.
- 103 C. Yi, J. Luo, S. Meloni, A. Boziki, N. Ashari-Astani, C. Grätzel, S. M. Zakeeruddin, U. Röthlisberger and M. Grätzel, *Energy Environ. Sci.*, 2016, **9**, 656–662.
- 104 J. S. Manser, J. A. Christians and P. V. Kamat, *Chem. Rev.*, 2016, **116**, 12956–13008.
- 105 W. Shockley and H. J. Queisser, *J. Appl. Phys.*, 1961, **32**, 510–519.
- 106 Y. Zhou, Z. Zhou, M. Chen, Y. Zong, J. Huang, S. Pang and N. P. Padture, *J. Mater. Chem. A*, 2016, **4**, 17623–17635.
- 107 Z. Xiao, Y. Zhou, H. Hosono, T. Kamiya and N. P. Padture, *Chem. - A Eur. J.*, 2018, **24**, 2305–2316.
- 108 T. C. Jellicoe, J. M. Richter, H. F. J. Glass, M. Tabachnyk, R. Brady, S. E. Dutton, A. Rao, R. H. Friend, D. Credgington, N. C. Greenham and M. L. Böhm, *J. Am. Chem. Soc.*, 2016, **138**, 2941–2944.
- 109 A. B. Wong, Y. Bekenstein, J. Kang, C. S. Kley, D. Kim, N. A. Gibson, D. Zhang, Y. Yu, S. R. Leone, L. W. Wang, A. P. Alivisatos and P. Yang, *Nano Lett.*, 2018, **18**, 2060–2066.

- 110 X. Wu, W. Song, Q. Li, X. Zhao, D. He and Z. Quan, *Chem. - An Asian J.*, 2018, **13**, 1654–1659.
- 111 K. Hills-Kimball, Y. Nagaoka, C. Cao, E. Chaykovsky and O. Chen, *J. Mater. Chem. C*, 2017, **5**, 5680–5684.
- 112 I. E. Castelli, J. M. García-Lastra, K. S. Thygesen and K. W. Jacobsen, *APL Mater.*, 2014, **2**, 081514.
- 113 W. Liu, Q. Lin, H. Li, K. Wu, I. Robel, J. M. Pietryga and V. I. Klimov, *J. Am. Chem. Soc.*, 2016, **138**, 14954–14961.
- 114 A. De, N. Mondal and A. Samanta, *Nanoscale*, 2017, **9**, 16722–16727.
- 115 W. J. Mir, M. Jagadeeswararao, S. Das and A. Nag, *ACS Energy Lett.*, 2017, **2**, 537–543.
- 116 D. Parobek, Y. Dong, T. Qiao and D. H. Son, *Chem. Mater.*, 2018, **30**, 2939–2944.
- 117 G. Huang, C. Wang, S. Xu, S. Zong, J. Lu, Z. Wang, C. Lu and Y. Cui, *Adv. Mater.*, 2017, **1700095**, 10–14.
- 118 G. Pan, X. Bai, D. Yang, X. Chen, P. Jing, S. Qu, L. Zhang, D. Zhou, J. Zhu, W. Xu, B. Dong and H. Song, *Nano Lett.*, 2017, **17**, 8005–8011.
- 119 D. Zhou, D. Liu, G. Pan, X. Chen, D. Li, W. Xu, X. Bai and H. Song, *Adv. Mater.*, 2017, **29**, 1–6.
- 120 T. Milstein, D. Kroupa and D. R. Gamelin, *Nano Lett.*, 2018, **18**, 3792–3799.
- 121 R. Begum, M. R. Parida, A. L. Abdelhady, B. Murali, N. M. Alyami, G. H. Ahmed, M. N. Hedhili, O. M. Bakr and O. F. Mohammed, *J. Am. Chem. Soc.*, 2017, **139**, 731–737.
- 122 K. Du, Q. Tu, X. Zhang, Q. Han, J. Liu, S. Zauscher and D. B. Mitzi, *Inorg. Chem.*, 2017, **56**, 9291–9302.
- 123 F. Meinardi, Q. A. Akkerman, F. Bruni, S. Park, M. Mauri, Z. Dang, L. Manna and S. Brovelli, *ACS Energy Lett.*, 2017, **2**, 2368–2377.
- 124 S. Zou, Y. Liu, J. Li, C. Liu, R. Feng, F. Jiang, Y. Li, J. Song, H. Zeng, M. Hong and X. Chen, *J. Am. Chem. Soc.*, 2017, **139**, 11443–11450.
- 125 S. Yang, F. Zhang, J. Tai, Y. Li, Y. Yang, H. Wang, J. Zhang, Z. Xie, B. Xu, H. Zhong, K. Liu and B. Yang, *Nanoscale*, 2018, **10**, 5820–5826.
- 126 L. Gomez, C. de Weerd, J. L. Hueso and T. Gregorkiewicz, *Nanoscale*, 2017, **9**, 631–636.
- 127 H. C. Wang, S. Y. Lin, A. C. Tang, B. P. Singh, H. C. Tong, C. Y. Chen, Y. C. Lee, T. L. Tsai and R. S. Liu, *Angew. Chemie - Int. Ed.*, 2016, **55**, 7924–7929.
- 128 D. N. Dirin, L. Protesescu, D. Trummer, I. V. Kochetygov, S. Yakunin, F. Krumeich, N. P. Stadie and M. V. Kovalenko, *Nano Lett.*, 2016, **16**, 5866–5874.
- 129 Q. A. Akkerman, S. Park, E. Radicchi, F. Nunzi, E. Mosconi, F. De Angelis, R. Brescia, P. Rastogi, M. Prato and L. Manna, *Nano Lett.*, 2017, **17**, 1924–1930.
- 130 S. K. Balakrishnan and P. V. Kamat, *Chem. Mater.*, 2018, **30**, 74–78.
- 131 F. Palazon, S. Dogan, S. Marras, F. Locardi, I. Nelli, P. Rastogi, M. Ferretti, M. Prato, R. Krahne and L. Manna, *J. Phys. Chem. C*, 2017, **121**, 11956–11961.
- 132 X. Peng, *Acc. Chem. Res.*, 2010, **43**, 1387–1395.
- 133 J. Park, H. Zheng, Y. Jun and A. P. Alivisatos, *J. Am. Chem. Soc.*, 2009, **131**, 13943–13945.
- 134 S. E. Creutz, E. N. Crites, M. C. De Siena and D. R. Gamelin, *Chem. Mater.*, 2018, **30**, 4887–4891.
- 135 D. M. Jang, K. Park, D. H. Kim, J. Park, F. Shojaei, H. S. Kang, J. P. Ahn, J. W. Lee and J. K. Song, *Nano Lett.*, 2015, **15**, 5191–5199.
- 136 B. A. Koscher, N. D. Bronstein, J. H. Olshansky, Y. Bekenstein and A. P. Alivisatos, *J. Am. Chem. Soc.*, 2016, **138**, 12065–12068.
- 137 D. Zhang, Y. Yang, Y. Bekenstein, Y. Yu, N. A. Gibson, A. B. Wong, S. W. Eaton, N. Kornienko, Q. Kong, M. Lai, A. P. Alivisatos, S. R. Leone and P. Yang, *J. Am. Chem. Soc.*, 2016, **138**, 7236–7239.
- 138 D. Parobek, Y. Dong, T. Qiao, D. Rossi and D. H. Son, *J. Am. Chem. Soc.*, 2017, **139**, 4358–4361.
- 139 C. Guhrenz, A. Benad, C. Ziegler, D. Haubold, N. Gaponik and A. Eychmüller, *Chem. Mater.*, 2016, **28**, 9033–9040.
- 140 V. K. Ravi, R. A. Scheidt, A. Nag, M. Kuno and P. V. Kamat, *ACS Energy Lett.*, 2018, **3**, 1049–1055.
- 141 Y. Xu, S. Xu, H. Shao, H. Jiang, Y. Cui and C. Wang, *Nanotechnology*, 2018, **29**, 235603.
- 142 D. Yu, B. Cai, F. Cao, X. Li, X. Liu, Y. Zhu, J. Ji, Y. Gu and H. Zeng, *Adv. Mater. Interfaces*, 2017, **4**, 1700441.
- 143 F. Li, Z. Xia, Y. Gong, L. Gu and Q. Liu, *J. Mater. Chem. C*, 2017, **5**, 9281–9287.
- 144 X. Fu, C. Zhang, Z. Peng, Y. Xia, J. Zhang, W. Luo, R. Zhan, H. Li, Y. Wang and D. Zhang, *J. Mater. Chem. C*, 2018, **6**, 1701–1708.
- 145 V. K. Ravi, P. K. Santra, N. Joshi, J. Chugh, S. K. Singh, H. Rensmo, P. Ghosh and A. Nag, *J. Phys. Chem. Lett.*, 2017, **8**, 4988–4994.
- 146 J. De Roo, M. Ibáñez, P. Geiregat, G. Nedelcu, W. Walravens, J. Maes, J. C. Martins, I. Van Driessche, M. V. Kovalenko and Z. Hens, *ACS Nano*, 2016, **10**, 2071–2081.
- 147 B. A. Koscher, J. K. Swabeck, N. D. Bronstein and A. P. Alivisatos, *J. Am. Chem. Soc.*, 2017, **139**, 6566–6569.
- 148 B. Luo, Y. C. Pu, S. A. Lindley, Y. Yang, L. Lu, Y. Li, X. Li and J. Z. Zhang, *Angew. Chemie - Int. Ed.*, 2016, **55**, 8864–8868.
- 149 B. Luo, S. B. Naghadeh, A. Allen, X. Li and J. Z. Zhang, *Adv. Funct. Mater.*, 2017, **27**, 1604018.
- 150 J. Pan, Y. Shang, J. Yin, M. De Bastiani, W. Peng, I. Dursun, L. Sinatra, A. M. El-Zohry, M. N. Hedhili, A.-H. Emwas, O. F. Mohammed, Z. Ning and O. M. Bakr, *J. Am. Chem. Soc.*, 2018, **140**, 562–565.
- 151 T. Udayabhaskararao, L. Houben, H. Cohen, M. Menahem, I. Pinkas, L. Avram, T. Wolf, A. Teitelboim, M. Leskes, O. Yaffe, D. Oron and M. Kazes, *Chem. Mater.*, 2018, **30**, 84–93.
- 152 J. B. Rivest and P. K. Jain, *Chem. Soc. Rev.*, 2013, **42**, 89–96.
- 153 T. Chiba, K. Hoshi, Y. J. Pu, Y. Takeda, Y. Hayashi, S. Ohisa, S. Kawata and J. Kido, *ACS Appl. Mater. Interfaces*, 2017, **9**, 18054–18060.
- 154 J. Pan, L. N. Quan, Y. Zhao, W. Peng, B. Murali, S. P. Sarmah, M. Yuan, L. Sinatra, N. M. Alyami, J. Liu, E. Yassitepe, Z. Yang, O. Voznyy, R. Comin, M. N. Hedhili, O. F. Mohammed, Z. H. Lu, D. H. Kim, E. H. Sargent and O. M. Bakr, *Adv. Mater.*, 2016, **28**, 8718–8725.
- 155 X. Zhang, Z. Jin, J. Zhang, D. Bai, H. Bian, K. Wang, J. Sun, Q. Wang and S. F. Liu, *ACS Appl. Mater. Interfaces*, 2018, **10**,

7145–7154.

156 S. H. Tolbert and A. P. Alivisatos, *J. Chem. Phys.*, 1995, **102**, 4642–4656.

157 J. N. Wickham, A. B. Herhold and A. P. Alivisatos, *Phys. Rev. Lett.*, 2000, **84**, 923–926.

158 Z. Wang, Y. Zhao, D. Schiferl, C. S. Zha, R. T. Downs and T. Sekine, *Appl. Phys. Lett.*, 2003, **83**, 3174–3176.

159 B. Li, K. Bian, X. Zhou, P. Lu, S. Liu, I. Brener, M. Sinclair, T. Luk, H. Schunk, L. Alarid, P. G. Clem, Z. Wang and H. Fan, *Sci. Adv.*, 2017, **3**, 1–8.

160 B. Li, X. Wen, R. Li, Z. Wang, P. G. Clem and H. Fan, *Nat. Commun.*, 2014, **5**, 4179.

161 Z. Wang, O. Chen, C. Y. Cao, K. Finkelstein, D.-M. Smilgies, X. Lu and W. A. Bassett, *Rev. Sci. Instrum.*, 2010, **81**, 093902.

162 H. Zhu, Y. Nagaoka, K. Hills-Kimball, R. Tan, L. Yu, Y. Fang, K. Wang, R. Li, Z. Wang and O. Chen, *J. Am. Chem. Soc.*, 2017, **139**, 8408–8411.

163 Y. Nagaoka, K. Hills-Kimball, R. Tan, R. Li, Z. Wang and O. Chen, *Adv. Mater.*, 2017, **29**, 1606666.

164 T. Yin, Y. Fang, W. K. Chong, K. T. Ming, S. Jiang, X. Li, J. L. Kuo, J. Fang, T. C. Sum, T. J. White, J. Yan and Z. X. Shen, *Adv. Mater.*, 2018, **30**, 1–8.

165 G. Xiao, Y. Cao, G. Qi, L. Wang, C. Liu, Z. Ma, X. Yang, Y. Sui, W. Zheng and B. Zou, *J. Am. Chem. Soc.*, 2017, **139**, 10087–10094.

166 J. C. Beimborn, L. M. G. Hall, P. Tongying, G. Dukovic and J. M. Weber, *J. Phys. Chem. C*, 2018, **122**, 11024–11030.

167 Y. Cao, G. Qi, C. Liu, L. Wang, Z. Ma, K. Wang, F. Du, G. Xiao and B. Zou, *J. Phys. Chem. C*, 2018, **122**, 9332–9338.

168 H. Zhu, T. Cai, M. Que, J.-P. Song, B. M. Rubenstein, Z. Wang and O. Chen, *J. Phys. Chem. Lett.*, 2018, **9**, 4199–4205.

169 X. Lü, Y. Wang, C. C. Stoumpos, Q. Hu, X. Guo, H. Chen, L. Yang, J. S. Smith, W. Yang, Y. Zhao, H. Xu, M. G. Kanatzidis and Q. Jia, *Adv. Mater.*, 2016, **28**, 8663–8668.

170 S. Jiang, Y. Fang, R. Li, H. Xiao, J. Crowley, C. Wang, T. J. White, W. A. Goddard, Z. Wang, T. Baikie and J. Fang, *Angew. Chemie Int. Ed.*, 2016, **55**, 6540–6544.

171 A. Jaffe, Y. Lin, C. M. Beavers, J. Voss, W. L. Mao and H. I. Karunadasa, *ACS Cent. Sci.*, 2016, **2**, 201–209.

172 L. Wang, K. Wang and B. Zou, *J. Phys. Chem. Lett.*, 2016, **7**, 2556–2562.

173 M. Szafranski and A. Katrusiak, *J. Phys. Chem. Lett.*, 2016, **7**, 3458–3466.

174 Y. Wang, X. Lü, W. Yang, T. Wen, L. Yang, X. Ren, L. Wang, Z. Lin and Y. Zhao, *J. Am. Chem. Soc.*, 2015, **137**, 11144–11149.

175 I. Swainson, L. Chi, J.-H. Her, L. Cranswick, P. Stephens, B. Winkler, D. J. Wilson and V. Milman, *Acta Crystallogr. Sect. B*, 2010, **66**, 422–429.

176 G. Liu, L. Kong, J. Gong, W. Yang, H. Mao, Q. Hu, Z. Liu, R. D. Schaller, D. Zhang and T. Xu, *Adv. Funct. Mater.*, 2017, **27**, 1604208.

177 L. Zhang, Q. Zeng and K. Wang, *J. Phys. Chem. Lett.*, 2017, **8**, 3752–3758.

178 L. Zhang, L. Wang, K. Wang and B. Zou, *J. Phys. Chem. C*, 2018, **122**, 15220–15225.

179 Y. Zong, Y. Zhou, Y. Zhang, Z. Li, L. Zhang, M.-G. Ju, M. Chen, S. Pang, X. C. Zeng and N. P. Padture, *Chem*, 2018, **4**, 1404–1415.

180 W. Q. Wu, Q. Wang, Y. Fang, Y. Shao, S. Tang, Y. Deng, H. Lu, Y. Liu, T. Li, Z. Yang, A. Gruverman and J. Huang, *Nat. Commun.*, 2018, **9**, 1–8.

181 P. W. Liang, C. Y. Liao, C. C. Chueh, F. Zuo, S. T. Williams, X. K. Xin, J. Lin and A. K. Y. Jen, *Adv. Mater.*, 2014, **26**, 3748–3754.

182 X. Li, M. Ibrahim Dar, C. Yi, J. Luo, M. Tschumi, S. M. Zakeeruddin, M. K. Nazeeruddin, H. Han and M. Grätzel, *Nat. Chem.*, 2015, **7**, 703–711.

183 C. Zuo and L. Ding, *Nanoscale*, 2014, **6**, 9935–9938.

184 M. Cha, P. Da, J. Wang, W. Wang, Z. Chen, F. Xiu, G. Zheng and Z.-S. Wang, *J. Am. Chem. Soc.*, 2016, **138**, 8581–8587.

185 H. Zai, C. Zhu, H. Xie, Y. Zhao, C. Shi, Z. Chen, X. Ke, M. Sui, C. Chen, J. Hu, Q. Zhang, Y. Gao, H. Zhou, Y. Li and Q. Chen, *ACS Energy Lett.*, 2017, **3**, 30–38.

186 J. Zhang, D. Bai, Z. Jin, H. Bian, K. Wang, J. Sun, Q. Wang and S. F. Liu, *Adv. Energy Mater.*, 2018, **8**, 1703246.

187 Q. Wang, X. Zhang, Z. Jin, J. Zhang, Z. Gao, Y. Li and S. F. Liu, *ACS Energy Lett.*, 2017, **2**, 1479–1486.

188 Y. Chen, L. Li, Z. Liu, N. Zhou, Q. Chen and H. Zhou, *Nano Energy*, 2017, **40**, 540–549.

189 W. H. Weber and J. Lambe, *Appl. Opt.*, 1976, **15**, 2299–2300.

190 F. Meinardi, A. Colombo, K. A. Velizhanin, R. Simonutti, M. Lorenzon, L. Beverina, R. Viswanatha, V. I. Klimov and S. Brovelli, *Nat. Photonics*, 2014, **8**, 392–399.

191 F. Purcell-Milton and Y. K. Gun'ko, *J. Mater. Chem.*, 2012, **22**, 16687–16697.

192 Z. Wang, Q. Lin, B. Wenger, M. G. Christoforo, Y.-H. Lin, M. T. Klug, M. B. Johnston, L. M. Herz and H. J. Snaith, *Nat. Energy*, 2018, In press, DOI:10.1038/s41560-018-0220-2.

193 G. E. Eperon, G. M. Paternò, R. J. Sutton, A. Zampetti, A. A. Haghghirad, F. Cacialli and H. J. Snaith, *J. Mater. Chem. A*, 2015, **3**, 19688–19695.

194 W. Ahmad, J. Khan, G. Niu and J. Tang, *Sol. RRL*, 2017, **1**, 1700048.

195 Q. Wang, X. Zheng, Y. Deng, J. Zhao, Z. Chen and J. Huang, *Joule*, 2017, **1**, 371–382.

196 P. Wang, X. Zhang, Y. Zhou, Q. Jiang, Q. Ye, Z. Chu, X. Li, X. Yang, Z. Yin and J. You, *Nat. Commun.*, 2018, **9**, 2225.

197 E. M. Sanehira, A. R. Marshall, J. A. Christians, S. P. Harvey, P. N. Ciesielski, L. M. Wheeler, P. Schulz, L. Y. Lin, M. C. Beard and J. M. Luther, *Sci. Adv.*, 2017, **3**, eaao4204.

198 L. M. Wheeler, E. M. Sanehira, A. R. Marshall, P. Schulz, M. Suri, N. C. Anderson, J. A. Christians, D. Nordlund, D. Sokaras, T. Kroll, S. P. Harvey, J. J. Berry, L. Y. Lin and J. M. Luther, *J. Am. Chem. Soc.*, 2018, **140**, 10504–10513.

199 Q. Wang, Z. Jin, D. Chen, D. Bai, H. Bian, J. Sun, G. Zhu, G. Wang and S. F. Liu, *Adv. Energy Mater.*, 2018, **8**, 1800007.

200 W. Travis, E. N. K. Glover, H. Bronstein, D. O. Scanlon and R. G. Palgrave, *Chem. Sci.*, 2016, **7**, 4548–4556.

201 H. Bian, D. Bai, Z. Jin, K. Wang, L. Liang, H. Wang, J. Zhang, Q. Wang and S. (Frank) Liu, *Joule*, 2018, **2**, 1500–1510.

## Journal Name

## ARTICLE

- 202 M. Leng, Y. Yang, K. Zeng, Z. Chen, Z. Tan, S. Li, J. Li, B. Xu, D. Li, M. P. Hautzinger, Y. Fu, T. Zhai, L. Xu, G. Niu, S. Jin and J. Tang, *Adv. Funct. Mater.*, 2018, **28**, 1704446.
- 203 Y. Lou, M. Fang, J. Chen and Y. Zhao, *Chem. Commun.*, 2018, **54**, 3779–3782.
- 204 J. S. Niezgodna, B. J. Foley, A. Z. Chen and J. J. Choi, *ACS Energy Lett.*, 2017, **2**, 1043–1049.
- 205 P. Reiss, M. Protière and L. Li, *Small*, 2009, **5**, 154–168.
- 206 O. Chen, J. Zhao, V. P. Chauhan, J. Cui, C. Wong, D. K. Harris, H. Wei, H.-S. Han, D. Fukumura, R. K. Jain and M. G. Bawendi, *Nat. Mater.*, 2013, **12**, 445–51.
- 207 M. V. Kovalenko, M. Scheele and D. V. Talapin, *Science*, 2009, **324**, 1417–1420.
- 208 Y. Yang, H. Qin, M. Jiang, L. Lin, T. Fu, X. Dai, Z. Zhang, Y. Niu, H. Cao, Y. Jin, F. Zhao and X. Peng, *Nano Lett.*, 2016, **16**, 2133–2138.
- 209 X. Chen, L. Peng, K. Huang, Z. Shi, R. Xie and W. Yang, *Nano Res.*, 2016, **9**, 1994–2006.
- 210 O. Chen, X. Chen, Y. Yang, J. Lynch, H. Wu, J. Zhuang and Y. C. Cao, *Angew. Chemie Int. Ed.*, 2008, **47**, 8638–8641.
- 211 K. Whitham, J. Yang, B. H. Savitzky, L. F. Kourkoutis, F. Wise and T. Hanrath, *Nat. Mater.*, 2016, **15**, 557–563.
- 212 J. J. Geuchies, C. van Overbeek, W. H. Evers, B. Goris, A. de Backer, A. P. Gantapara, F. T. Rabouw, J. Hilhorst, J. L. Peters, O. Konovalov, A. V. Petukhov, M. Dijkstra, L. D. A. Siebbeles, S. van Aert, S. Bals and D. Vanmaekelbergh, *Nat. Mater.*, 2016, **15**, 1248–1254.
- 213 M. Cargnello, A. C. Johnston-Peck, B. T. Diroll, E. Wong, B. Datta, D. Damodhar, V. V. T. Doan-Nguyen, A. A. Herzing, C. R. Kagan and C. B. Murray, *Nature*, 2015, **524**, 450–453.
- 214 D. Han, M. Imran, M. Zhang, S. Chang, X. Wu, X. Zhang, J. Tang, M. Wang, S. Ali, X. Li, G. Yu, J. Han, L. Wang, B. Zou and H.-Z. Zhong, *ACS Nano*, 2018, In press, DOI: acsnano.8b05172.



Halide Perovskite Nanocrystals



Perovskite Solar Cell Device

Perspectives on how halide perovskite nanocrystals are better integrated in perovskite solar cells are provided.